SIMULATION OF A SLACK-MOORED HEAVING-BUOY WAVE-ENERGY CONVERTER WITH PHASE CONTROL

by

Håvard Eidsmoen

Division of Physics
Norwegian University of Science and Technology
N-7034 Trondheim
Norway

May 1996

Abstract

A mathematical model is presented for a slack-moored wave-energy converter (WEC), consisting of a semi-submerged heaving buoy moving relative to a submerged plate. For the WEC investigated the diameter of the cylindrical buoy is 3.3 m and the cylinder ends are, at equilibrium, 3.1 m below mean water level and 2.0 m above. The plate has diameter 8.0 m, is 0.2 m thick and is submerged 10 m. The geometry is chosen so that the heave excitation forces on the two bodies are approximately equal in magnitude, but in opposite direction, for wave periods we want to absorb energy from. A high-pressure hydraulic machinery is proposed for energy production and motion control. A valve in the machinery can be actively controlled, and it is used to obtain largest possible power production, and to limit the excursion of the buoy, in order to protect the hydraulic machinery. In addition, an end-stop device is provided as a safety measure, in case the control fails to limit the excursion.

A procedure is developed for control of the device in both sinusoidal and irregular waves. This procedure determines the opening instant of the controllable valve so that, in small waves the extrema of the relative velocity between the bodies coincide with the extrema of the excitation force, while in larger waves the opening instant is delayed to constrain the excursion. The control procedure is also used to keep the plate in the desired mean position, since the submerged body has no hydrostatic stiffness.

Results are presented for calculations with sinusoidal waves, and irregular waves based on a Pierson-Moskowitz spectrum. In sinusoidal waves the energy production is largest for waves with period 4 s and 5 s. The control procedure is not totally successful, since the mean position of the piston is usually negative for long wave periods, and the full length of the available piston stroke is not utilised. In irregular waves the power production has an approximately linear increase with the significant wave height. The control procedure is not able to constrain the excursion sufficiently, so the end-stop device is engaged too often. The excursion of the piston does also here usually have a negative mean value, which means that the available piston stoke is not fully utilised. By further development of the control procedure it should be possible to solve these problems, and at the same time increase the power production.

On the basis of a scatter table, for a wave climate where the average incident wave power per unit width is approximately 37 kW/m, the year-average power production is estimated to be approximately 4.9 kW. However, the size of the device is relatively small for the wave climate investigated. Further, a duration curve is presented, which shows the percentage of the year the mean power production is above a certain level.

List of symbols

The most frequently used symbols are presented in the following list. SI units are included in brackets. The derivative of a variable with respect to time is denoted by a dot above the variable.

A_D	[m^2]	Cross sectional area of the plate perpendicular to the z-axis
A_o	[m^2]	Orifice area of valves
A_p	[m^2]	Net area of hydraulic piston
A_w	[m^2]	Water plane area of buoy ($A_w = \pi D_b^2/4$)
B_-	[kg/m]	Constant for damping term of the end-stop force
B_+	[kg/m]	Constant for damping term of the end-stop force
C_D		Drag coefficient of the plate
D_b	[m]	Diameter of buoy
D_p	[m]	Diameter of plate
f_b	[kg/s^3]	Excitation force kernel of the buoy
f_p	[kg/s^3]	Excitation force kernel of the plate
F_c	[N]	Force from the end-stop device
F_{drag}	[N]	Non-linear drag force on plate
$F_{e,b}$	[N]	Excitation force on buoy
$F_{e,p}$	[N]	Excitation force on plate
$F_{f,b}$	[N]	Linear friction force on buoy
$F_{f,p}$	[N]	Linear friction force on plate
F_m	[N]	Net buoyancy force on buoy submerged to equilibrium position
$F_{r,b}$	[N]	Radiation force on buoy
$F_{r,p}$	[N]	Radiation force on plate
F_u	[N]	Force from hydraulic system on buoy (and plate)
$F_{w,b}$	[N]	Total wave force on the buoy, $F_{w,b} = F_{e,b} + F_{r,b}$
$F_{w,p}$	[N]	Total wave force on the plate, $F_{w,p} = F_{e,p} + F_{r,p}$
g	[m/s^2]	Acceleration of gravity
h	[m]	Water depth
H	[m]	Wave height
H_s	[m]	Significant wave height
I_{int}	[Ns]	Integral of excitation force used in control strategy
I_{max}	[Ns]	Variable parameter used in control strategy
I_{min}	[Ns]	Variable parameter used in control strategy
k	[m^{-1}]	Angular repetency (wave number)
k_-	[N/m]	Constant for spring term of the end-stop force
k_+	[N/m]	Constant for spring term of the end-stop force
k_{11}	[kg/s^2]	Integration kernel for the radiation force on the buoy due to the motion of the buoy
$k_{12} = k_{21}$	[kg/s^2]	Integration kernel for the radiation force on the buoy due to the motion of the plate, and for the radiation force on the plate due to the motion of the buoy
k_{22}	[kg/s^2]	Integration kernel for the radiation force on the plate due to the

		motion of the plate
$m_{r,11}(\infty)$	[kg]	Added mass of the buoy at infinite frequency
$m_{r,12}(\infty)$	[kg]	Added mass of the buoy due to the motion of the plate, at infinite frequency
$m_{r,21}(\infty)$	[kg]	Added mass of the plate due to the motion of the buoy, at infinite frequency
$m_{r,22}(\infty)$	[kg]	Added mass of the plate at infinite frequency
m_b	[kg]	Mass of buoy
m_p	[kg]	Mass of plate
p	[Pa]	Pressure
p_{max}	[Pa]	Maximum pressure in cylinder
p_{min}	[Pa]	Minimum pressure in cylinder
p_A	[Pa]	Pressure in gas accumulator *A*
p_B	[Pa]	Pressure in gas accumulator *B*, high pressure accumulator
p_C	[Pa]	Pressure in gas accumulator *C*, low pressure accumulator
p_D	[Pa]	Pressure in gas accumulator *D*, equal to cylinder pressure
P	[W]	Power
P_{drag}	[W]	Mean power dissipated due to the non-linear drag force
P_l	[W]	Mean power lost in the hydraulic machinery (valves)
P_u	[W]	Mean power produced by the hydraulic machinery
Q	[m^3/s]	Flow rate or flow per unit time
Q_m	[m^3/s]	Mean flow through hydraulic motor
Q_{max}	[m^3/s]	Maximum flow through hydraulic motor
$R_{f,b}$	[kg/s]	Friction resistance of buoy
$R_{f,p}$	[kg/s]	Friction resistance of plate
R_{11}	[kg/s]	Radiation resistance of the buoy due to the motion of the buoy
R_{12}	[kg/s]	Radiation resistance of the buoy due to the motion of the plate
R_{21}	[kg/s]	Radiation resistance of the plate due to the motion of the buoy
R_{22}	[kg/s]	Radiation resistance of the plate due to the motion of the plate
s_b	[m]	Heave excursion of buoy, from equilibrium
s_{max}	[m]	Maximum excursion of piston relative to cylinder (plate relative to buoy), in positive direction from equilibrium
s_{min}	[m]	Maximum excursion of piston relative to cylinder (plate relative to buoy), in negative direction from equilibrium
s_p	[m]	Heave excursion of plate, from equilibrium
s_-	[m]	Design limit for excursion of the piston, in negative direction. Excursion at which the end-stop device is engaged.
s_+	[m]	Design limit for excursion of the piston, in positive direction. Excursion at which the end-stop device is engaged.
S_b	[N/m]	Hydrostatic stiffness of buoy ($S_b = \rho g A_w$)
t	[s]	Time
T	[s]	Wave period
T_0	[s]	Natural period of buoy
T_{pred}	[s]	Prediction time for excitation force
T_z	[s]	Zero-upcross period
u_b	[m/s]	Heave velocity of buoy, equal to $\dot{s}_b$

u_p	[m/s]	Heave velocity of plate, equal to $\dot{s}_p$
V	[m^3]	Volume
V_b	[m^3]	Submerged volume of buoy in equilibrium position
V_A	[m^3]	Gas volume of accumulator *A*
V_B	[m^3]	Gas volume of accumulator *B*, high pressure accumulator
V_C	[m^3]	Gas volume of accumulator *C*, low pressure accumulator
V_D	[m^3]	Gas volume of accumulator *D*
γ		Ratio of the specific heat capacities
η	[m]	Wave elevation
μ		Discharge coefficient of orifice
ρ	[kg/m^3]	Density of water
ρ_o	[kg/m^3]	Density of oil
ω	[rad/s]	Angular frequency

1 Introduction

One of the main problems with the heaving-buoy wave-energy converter (WEC) is to establish a reference against which the conversion mechanism can work. The most obvious reference is a strut connected to the ocean floor, a fixed reference. This will, however, be a relatively expensive construction, with a long strut exposed to large bending moments, a universal joint and an anchor. Further, some kind of compensation mechanism must be included in the design if the tidal range is large, and this design is necessarily restricted to relatively shallow water. An alternative to this is to use a submerged body as a reference, and apply a conversion mechanism which utilise the relative motion between the two bodies. The WEC can then be slack-moored, and the mooring is used to keep the WEC in the desired horizontal position. A proposal has been put forward, where the bodies are designed in such a way that the vertical wave excitation force on the floating body is compensated by the excitation force on the submerged body, for wave periods we want to absorb energy from.[1] That is, the heave excitation forces are approximately equal in magnitude, but in opposite direction. In the largest waves, with relatively long period, both bodies follow the waves, and the WEC is exposed to lower loads than a tight-moored device. This kind of reference might in the long run turn out to be the most practical and economical solution. The present work with a slack-moored device is an extension of previous work with tight-moored devices,[2] and is an attempt of determining a practical design for the geometry and the power take-off system.

For WECs of this design it is essential that means are provided for optimum control of the oscillatory motion, in order to achieve maximum power conversion. So far, optimum control has mainly been considered with sinusoidal waves,[3,4,5,6,7,8,9] but also irregular waves have been considered.[9,10,11,12,13] The purpose of the control is then to obtain optimum phase and optimum amplitude of the oscillation in order to maximise the converted power. Linear theory will, in general, give simple frequency-domain expressions for the optimum condition. However, it is inherent with the design of a WEC that there is an upper bound on the oscillation amplitude. Moreover, the energy-converting device has a limited power capacity. The optimum conditions will then depend on whether or not the oscillation amplitude is constrained. When the equation of motion becomes non-linear, as it does when the amplitude is constrained, the frequency-domain description becomes less suitable, and the optimisation must be carried out in the time domain, for instance by optimum control theory.[9,14,15,16,17,18] It is then more difficult to give simple expressions for the optimum conditions. Moreover, when the incident wave is very large, we might want to control the WEC so that the power is within the capacity of the machinery, and so that the loads on the WEC are as small as possible. An additional complication in the present work is that a two-body problem is being studied, while most problems studied previously have been for a single body.

In the present text it is focused on discussing the general principles on how to approach optimum, and a design is proposed in order to implement the control in practice. A mathematical model is presented for a WEC, consisting of a floating buoy moving relative to a submerged plate, and the WEC is, in general, exposed to an irregular incident wave. The buoy is interconnected to the plate by a piston-and-cylinder, exerting a force on both bodies. The cylinder is connected to a high-pressure hydraulic system, which is used

for energy storage and production of useful energy. The hydraulic system has some components which can be actively controlled. This makes it possible to control the pressure in the cylinder and thereby the relative motion of the two bodies. In the present text oscillation in heave only is considered. It should be noted that, since the system is axisymmetric, it is possible for this system to absorb power equal to the incident power of a wave front of width equal to the wavelength divided by 2π, when the oscillation is unconstrained.[19]

The aim of the present work is to investigate (real time) procedures which control the motion of the WEC so that as much energy as possible is produced by the conversion machinery, while they at the same time protect the hydraulic piston-and-cylinder by limiting the relative excursion between the bodies. The control procedure is also used to keep the submerged body in the desired mean position, since the submerged body has no hydrostatic stiffness. To do this the general principles on how to obtain optimum must be addressed, and the control strategy must be implemented through the control of the hydraulic system. Further, the hydraulic system must be designed so that it, in a best possible way, can realise the control strategy. These problems are investigated by time-domain simulations of the WEC.

When optimum control is considered in irregular waves it is necessary to predict the incident wave. This means that the control strategy is non-causal. How long time into the future it is necessary to predict the incident wave will depend on the control strategy, and on the size of the device. If the prediction of the incident wave is imperfect, the optimum motion can be realised only approximately.

2 Mathematical model

2.1 The forces

We consider a WEC in the form of a heaving buoy, oscillating relative to a submerged plate. In general, the geometry of the device and of the surrounding submerged solid boundaries is arbitrary, and influences the problem only through the hydrodynamic parameters of the device. The waves incident to the device are, in general, irregular. The total wave force on the buoy can be written as

$$F_{w,b}(t) = F_{e,b}(t) + F_{r,b}(t) \tag{1}$$

and similarly for the plate, but with sub-index p instead of b.

The excitation force is given by

$$F_{e,b}(t) = f_b(t) * \eta(t) = \int_{-\infty}^{\infty} \eta(\tau) f_b(t-\tau) d\tau \tag{2}$$

which is a convolution product. Here $\eta(t)$ is the surface elevation due to the incident wave at the origin and $f_b(t)$ is the excitation force kernel of the buoy. The excitation force on the plate can similarly be computed from the excitation force kernel for the plate, $f_p(t)$. An example of the two excitation force kernels, for the geometry shown in figure 1, is given

in figure 2. The radiation forces on the two bodies are given by [20]

$$\begin{aligned} F_{r,b}(t) &= -m_{r,11}(\infty)\dot{u}_b(t) - \int_{-\infty}^{t} k_{11}(t-\tau)u_b(\tau)d\tau - m_{r,12}(\infty)\dot{u}_p(t) - \int_{-\infty}^{t} k_{12}(t-\tau)u_p(\tau)d\tau \\ &= -m_{r,11}(\infty)\dot{u}_b(t) - k_{11}(t) * u_b(t) - m_{r,12}(\infty)\dot{u}_p(t) - k_{12}(t) * u_p(t) \\ F_{r,p}(t) &= -m_{r,21}(\infty)\dot{u}_b(t) - \int_{-\infty}^{t} k_{21}(t-\tau)u_b(\tau)d\tau - m_{r,22}(\infty)\dot{u}_p(t) - \int_{-\infty}^{t} k_{22}(t-\tau)u_p(\tau)d\tau \\ &= -m_{r,21}(\infty)\dot{u}_b(t) - k_{21}(t) * u_b(t) - m_{r,22}(\infty)\dot{u}_p(t) - k_{22}(t) * u_p(t) \end{aligned} \tag{3}$$

where $m_{r,ij}(\infty)$ ($i = 1,2$, $j = 1,2$) are the elements of the added mass matrix of the WEC, at infinite frequency, $u_b(t)$ and $u_p(t)$ are the vertical velocities of the two bodies, $\dot{u}_b(t)$ and $\dot{u}_p(t)$ are the vertical accelerations and $k_{ij}(t)$ ($i = 1,2$, $j = 1,2$) are the radiation force kernels. An example of radiation force kernels, for the geometry shown in figure 1, is given in figure 3. Note that, in equation (3), the upper integration limits are t because the radiation force kernels, contrary to the excitation force kernels, are causal impulse response functions, that is $k_{ij}(t) = 0$ for $t < 0$. Further, we have $k_{12}(t) = k_{12}(t)$, due to the symmetry of the radiation resistance matrix. The integration kernels have been obtained from the frequency domain expressions for the hydrodynamic parameters of the body, which have been computed by a method previously described by the author, using linear hydrodynamic theory and assuming an ideal incompressible fluid.[19] The calculation is described in more detail in Appendix A. Note that, since the kernels are computed by linear hydrodynamic theory, these expressions are valid only for small excursions. How large the error becomes when the excursion is large, depends on the geometry of the device and of the steepness of the incident wave.

A linear friction loss force is also included, and we choose to write

$$F_{f,b}(t) = -R_{f,b}\, u_b(t) \tag{4}$$

for the buoy, and a similar expression is used for the plate. The friction resistance consists of contributions from viscous friction, mechanical friction, and conversion losses in the machinery. The friction resistances, $R_{f,b}$ and $R_{f,p}$, are for simplicity assumed to be independent of the oscillation amplitude and of the frequency.

A non-linear drag force is included on the submerged body. This is expected to be the most important non-linear hydrodynamic force, due to the geometry of the plate. The drag force is expressed as follows [21]

$$F_{drag}(t) = -\frac{C_D}{2}\rho A_D \left|u_p(t)\right| u_p(t) \tag{5}$$

Where A_D is the cross sectional area of the plate perpendicular to the direction of the motion, and C_D is the drag coefficient. The drag coefficient for plates has been investigated by Keulegan and Carpenter.[22] Note the absolute value of one of the velocity terms, ensuring that the force is always in the opposite direction to the velocity. This expression would have been more realistic if the velocity of the plate relative to the water particles had

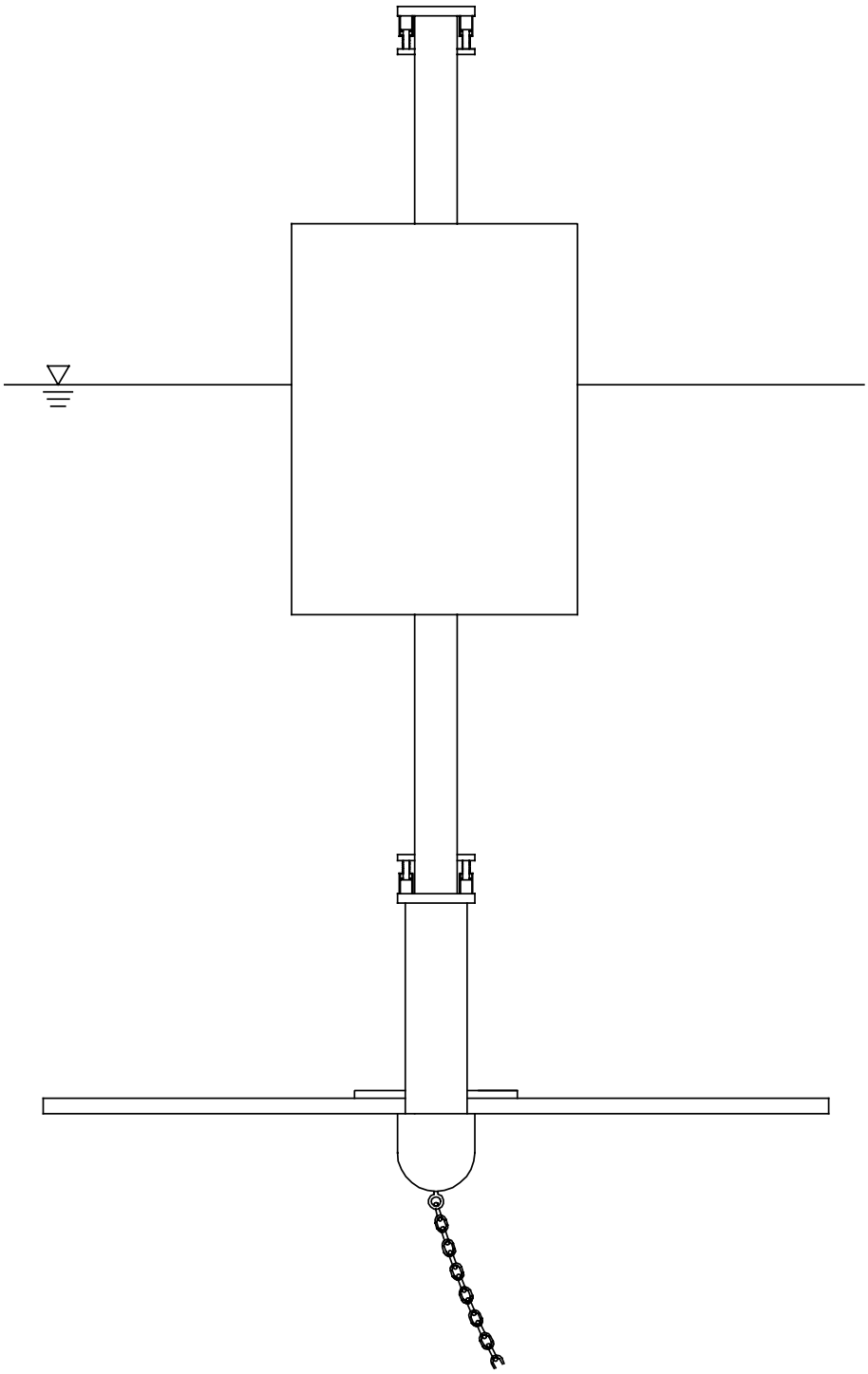

Figure 1. *Sketch of the geometry of the WEC. The diameter of the buoy is 3.3 m and the height is 5.1 m, of which 3.1 m is submerged at equilibrium. The diameter of the plate is 8 m, the thickness is 0.2 m and the submergence is 10.0 m.*

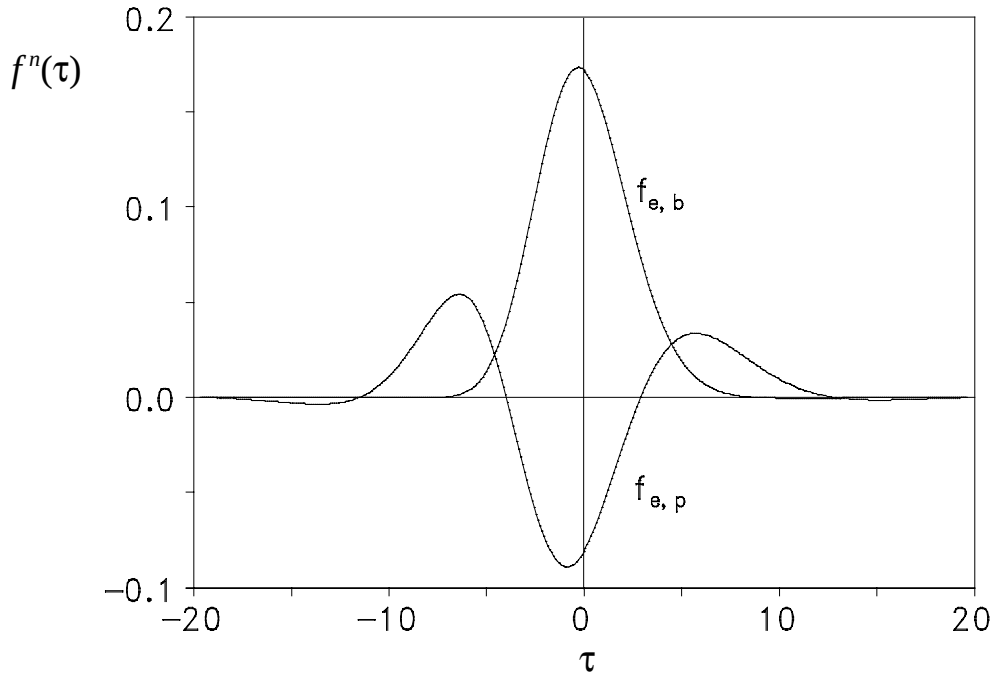

Figure 2. *The non-dimensional heave excitation force kernels* $f^n(\tau) = f(t)(D_b/(2g))^{1/2}/S_b$ *versus the non-dimensional time,* $\tau = (2g/D_b)^{1/2}t$*, for the geometry described in figure 1.*

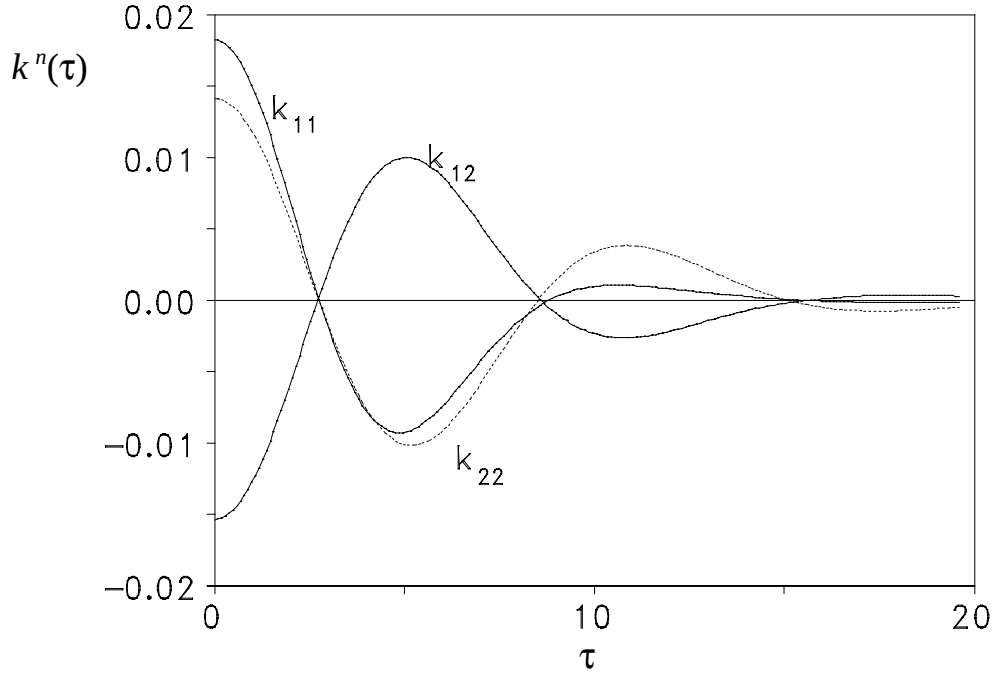

Figure 3. *The non-dimensional heave radiation force kernels* $k^n(\tau) = k(t)/S_b$ *versus the non-dimensional time,* $\tau = (2g/D_b)^{1/2}t$*, for the geometry described in figure 1. Note that all* $k(t) = 0$ *for* $t < 0$*. The calculation was, in this case, stopped for* $\tau \approx 19$*.*

been used instead of the velocity of the plate. However, it would be almost impossible to compute the velocity of the water particles, since the flow around the plate is very complex in an irregular wave.

The WEC is equipped with a hydraulic machinery which produces a load force $F_u(t)$, which is given by the pressure difference across the piston multiplied by the net piston area. The load force (which also includes a pretension force to balance the force F_m described below) is working between the two bodies, and is taken to be positive when it is acting on the buoy in the positive z-direction. Thus, $F_u(t)$ is negative when there is a tension force in the piston rod. The hydraulic system investigated, which is also used to produce useful energy, is described in Appendix B and shown in figure 4.

The net buoyancy of the buoy, that is the difference between the buoyancy and the weight of the buoy at the equilibrium position, is given by

$$F_m = g(\rho V_b - m_b) \tag{6}$$

where V_b is the submerged volume of the buoy at equilibrium and m_b the mass of the body. The net buoyancy of the submerged plate has the same magnitude, but opposite sign, so that the total net buoyancy of the WEC is zero. This force is transferred between the bodies through the hydraulic system. That is, in the equilibrium position the force on the buoy from the hydraulic system is $-F_m$, and the force on the plate is F_m.

For a real WEC the excursion has to be limited, for instance because of the finite length of hydraulic rams. It is often necessary to include a deceleration cushion at the end of the stroke, and this function is carried out by the end-stop device. This device dissipates kinetic energy of the load gently, and reduces the possibility of mechanical damage to the cylinder. The force from the end-stop device is denoted $F_c(t)$, and might include both damping terms and spring terms. The excursion at which the end-stop is engaged, is, in the following, termed the design limit of the excursion. A more detailed description of this force is given in Appendix C.

2.2 The equation of motion

The equations of motion for the two bodies may now be written as follows, when the forces described in the previous chapter are included,

$$\begin{aligned} m_b\ddot{s}_b(t) + S_b s_b(t) &= F_{w,b}(t) + F_{f,b}(t) + F_u(t) + F_c(t) + F_m \\ m_p\ddot{s}_p(t) &= F_{w,p}(t) + F_{f,p}(t) - F_u(t) - F_c(t) - F_m + F_{drag}(t) \end{aligned} \tag{7}$$

where s_b and s_p are the vertical distances of displacement from equilibrium for the buoy and the plate, m_b and m_p are the masses of the bodies and $S_b = \rho g A_w$ is the hydrostatic stiffness of the buoy, A_w being the water plane area. We choose to consider S_b as constant, not depending on the excursion, which is correct for a vertical cylinder. These equations can be reorganised as follows

$$\begin{aligned} (m_b + m_{r,11}(\infty))\dot{u}_b(t) + m_{r,12}(\infty)\dot{u}_p(t) &= g_1(t) \\ m_{r,21}(\infty)\dot{u}_b(t) + (m_p + m_{r,22}(\infty))\dot{u}_p(t) &= g_2(t) \end{aligned} \tag{8}$$

when the expressions for the radiation forces given in equation (3) have been used, and the following functions have been introduced to increase the readability

$$\begin{aligned} g_1(t) &= F_{e,b}(t) - k_{11}(t) * u_b(t) - k_{12}(t) * u_p(t) - R_{f,b}\, u_b(t) - S_b\, s_b(t) + F_u(t) + F_c(t) + F_m \\ g_2(t) &= F_{e,p}(t) - k_{21}(t) * u_b(t) - k_{22}(t) * u_p(t) - R_{f,p}\, u_p(t) - F_u(t) - F_c(t) - F_m + F_{drag}(t) \end{aligned} \tag{9}$$

By further manipulation the equations of motion can be written as the following system of equations

$$\begin{aligned} \dot{s}_b(t) &= u_b(t) \\ \dot{u}_b(t) &= C_{11} g_1(t) + C_{12} g_2(t) \\ \dot{s}_p(t) &= u_p(t) \\ \dot{u}_p(t) &= C_{21} g_1(t) + C_{22} g_2(t) \end{aligned} \tag{10}$$

which are also called state equations. The following constants have been introduced

$$\begin{aligned} C_{11} &= (m_b + m_{r,11}(\infty))^{-1}\left(1 - \frac{m_{r,12}(\infty) m_{r,21}(\infty)}{(m_b + m_{r,11}(\infty))(m_p + m_{r,22}(\infty))}\right)^{-1} \\ C_{12} &= -\frac{m_{r,12}(\infty)}{(m_b + m_{r,11}(\infty))(m_p + m_{r,22}(\infty))}\left(1 - \frac{m_{r,12}(\infty) m_{r,21}(\infty)}{(m_b + m_{r,11}(\infty))(m_p + m_{r,22}(\infty))}\right)^{-1} \\ C_{21} &= -\frac{m_{r,21}(\infty)}{(m_b + m_{r,11}(\infty))(m_p + m_{r,22}(\infty))}\left(1 - \frac{m_{r,12}(\infty) m_{r,21}(\infty)}{(m_b + m_{r,11}(\infty))(m_p + m_{r,22}(\infty))}\right)^{-1} \\ C_{22} &= (m_p + m_{r,22}(\infty))^{-1}\left(1 - \frac{m_{r,12}(\infty) m_{r,21}(\infty)}{(m_b + m_{r,11}(\infty))(m_p + m_{r,22}(\infty))}\right)^{-1} \end{aligned} \tag{11}$$

3 The computer program

The main purpose of the computer program, which has been developed, is to carry out an integration of the equations of motion (10). This is done by a fourth order Runge-Kutta procedure[23] with variable step length. The procedure advances the solution through a time interval of predetermined length, first by one step and afterwards the interval is divided into two time steps. The two solutions obtained for the excursion at the end of the interval are compared, and if the difference is below a given value the solution is accepted. If the discrepancy is too large, the number of time steps is doubled and the integration is repeated. This procedure is repeated until the discrepancy between the two solutions with the largest number of time steps is below the given value. The procedure then moves on to advance the solution through the next time interval.

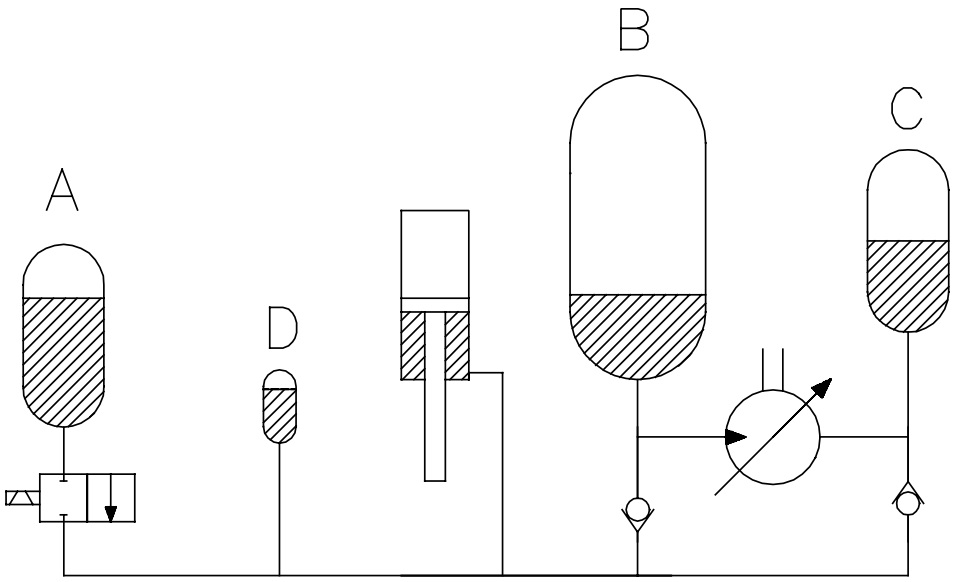

Figure 4. *Sketch of the hydraulic system proposed for WEC. The cylinder is connected to the buoy and the piston is connected to the plate. The system is described in more detail in Appendix B.*

The convolution integrals for the excitation forces (2) and the radiation forces (3) are evaluated by a trapezoidal approximation, where the time step equals the length of the predetermined intervals with which the equation of motion is advanced, and the values are determined in both ends of each interval. This is done to reduce the computing time and the requirement for storage of previous values of the solution. Interpolation by splines is used to obtain values inside the intervals. Further, the integrations are truncated in order to reduce the computing time. From figure 2 and 3 we see that this is an assumption which is easy to justify, since the integration kernels tend fast to zero as $|t| \to \infty$.

The surface elevation of the incident wave is read from a file with a certain sampling time, and spline interpolation is used to determine the wave elevation between the samples, if necessary.

The pressure in the cylinder, and thereby the force from the piston-and-cylinder on the buoy, is determined as follows. A gas accumulator (labelled *D*) is connected directly to the cylinder, as shown if figure 4, and the pressure in this accumulator is assumed to be the same as in the cylinder. The flow between the accumulators, and thereby the oil volume and pressure in the accumulators, are determined by the flow through the valves and by the motion of the piston. The system of pipes connecting the accumulators is assumed to be of minor importance. The equations used to relate the pressures, volumes and flows are described in Appendix B.

For each time step in the solution of the equation of motion, a procedure, that perhaps

can best be termed as a Euler-algorithm, is used to advance the solution for the hydraulic system, using several shorter time steps. The flow through each of the valves is determined at the beginning of each time step, and assumed to be constant during the time step, not taking into account the pressure change during this time interval. However, in some cases analytical solutions are used within the procedure. From the flow through the valves and the motion of the piston, the gas volumes and pressures of the accumulators are determined at the end of the time step. The number of time steps used by the procedure has a minimum value, and the number is increased if, during one particular time step, the pressure change in the cylinder is above a given value. This is done to reduce the computing time, and at the same time get an acceptable accuracy for the solution.

4 Summary of results

Calculations have been carried out for the WEC shown in figure 1, with the hydraulic system described in Appendix B and shown in figure 4. The diameter of the cylindrical buoy is 3.3 m and the cylinder ends are, at equilibrium, 3.1 m below mean water level and 2.0 m above. The plate has diameter 8.0 m, is 0.2 m thick and is submerged 10 m. The shape of the buoy and plate is chosen for mathematical convenience, and a real WEC should not have sharp edges. The mass of the buoy is $9.7 \cdot 10^3$ kg. This means that the force from the hydraulic system, acting on the buoy, in the equilibrium position, is 173 kN downwards, and the net buoyancy force is 173 kN upwards. The mass of the plate is $28 \cdot 10^3$ kg, giving a net buoyancy force which is 173 kN downwards. In the equilibrium position this force is balanced by the force from the hydraulic system. During operation there should always be tension in the piston rod. The friction resistances are set to $R_{f,b} = R_{f,p} = 200$ Ns/m, and the drag coefficient on the plate is chosen to be $C_D = 10$. This corresponds to approximately 10% of the maximum radiation resistance of the two bodies. The excitation force kernels and the radiation force kernels for this geometry are given in figure 2 and 3, for water depth $h = 25$ m. It has further been assumed that the elements of the added mass matrix at infinite frequency are approximately $m_{r,11}(\infty) = 8.7 \cdot 10^3$ kg, $m_{r,12}(\infty) = m_{r,21}(\infty) = -8 \cdot 10^3$ kg and $m_{r,22}(\infty) = 190 \cdot 10^3$ kg. The frequency-domain hydrodynamic parameters of the device have been computed by a method previously described by the author,[19] and a more detailed description of the calculation is given in Appendix A. The hydraulic cylinder is envisaged to be 5.0 m long, 2.5 m in each direction from the equilibrium position of the piston. However, the length of the cylinder does not enter into the mathematical model, and the calculation results are not incorrect if the excursion exceeds 2.5 m. The piston has a stroke of 2 m in each direction, from the equilibrium position, before the end-stop device comes into operation. This is the design limit of the excursion. The maximum time step used for the integration of the equation of motion is 0.04 s, and the integration kernels are assumed to be zero for $|t| > 8.0$ s (corresponding to non-dimensional time $\tau = 19$ in figure 2 and 3). A summary of values of constants and initial values of variables used in the calculations, is given in table 1 and table 2.

Constants			
A_o	0.0079 m^2	$m_{r,22}(\infty)$	190000 kg
A_p	0.0173 m^2	$R_{f,b}$	200 kg/s
$B_- = B_+$	9200 kg/m	$R_{f,p}$	200 kg/s
C_D	10	S_b	86.4 kN/m
D_b	3.3 m	s_+	2.0 m
D_p	8.0 m	s_-	-2.0 m
F_m	173 kN	T_0	2.2 s
g	9.81 m/s^2	T_{pred}	4.4 s
h	25 m	V_b	26.5 m^3
$k_- = k_+$	50 kN/m	γ	1.4
m_b	9700 kg	μ	0.611
m_p	28000 kg	ρ	1030 kg/m^3
$m_{r,11}(\infty)$	8700 kg	ρ_o	850 kg/m^3
$m_{r,12}(\infty)$	-8000 kg		

Table 1. Values of constants used in the calculations, for both systems.

p_A	10 MPa	V_A	0.30 m^3
p_B	13 MPa	V_B	0.52 m^3
p_C	7 MPa	V_C	0.092 m^3
p_D	10 MPa	V_D	0.0005 m^3

Table 2. *Initial values of variables used in the calculations.*

4.1 Regular waves

Calculations have been carried out for a number of combinations of wave period and wave height, with sinusoidal incident waves. To avoid problems with transient motions when starting the calculation, the wave height is gradually increased from zero to the desired value, and then held at this value for the rest of the wave series. Further, the calculation is not stopped before a steady periodic solution has been obtained for five to ten periods.

In order to test the numerical procedure, calculations were performed for a system where an analytical solution could be obtained. In this case the hydraulic system was replaced by a linear spring force and linear damping force, and the non-linear drag force

was not included. The numerical and the analytical solutions were found to be in good agreement.

Calculations have been carried out for sinusoidal waves to determine how the buoy should be controlled to obtain maximum power production when the excursion is limited to ±2.0 m. That is, the end-stop device should not come into operation. It would then be desirable to determine the optimum opening instant of the controllable valve, for each wave height and period. However, the submerged body does not have a hydrostatic stiffness, so there is no hydrostatic force which returns it to the desired equilibrium position. This makes the analysis more complex than for a tight-moored device, where the buoy is pulled back to the equilibrium position by the hydrostatic force. This means that in addition to determining the optimum opening instant for the controllable valve, it is necessary to actively control the position of the submerged body, so that it does not move too far in either direction. Carrying out this process for each combination of wave height and period would be very time consuming, and in the present calculations the same control procedure has been used to determine the opening instant for all wave heights and periods. This control procedure is described in Appendix D. The control procedure used here has the excitation force as input, and contains some design-specific parameters, which have been determined by running the program several times, for different sea states. The parameters were changed to maximise the power production, and at the same time keep the excursion within the design limits and the mean position of the submerged body as close as possible to the equilibrium position.

Table 3 and figure 5 show the mean power production, P_u, neglecting energy losses in the hydraulic motor. We observe that the power production is largest for waves with period 4 s and 5 s. For the longest wave periods the motion of the plate follows the motion of the buoy, and the pressure necessary to open the check valves in the hydraulic system is established only in short intervals. This results in a relatively low energy production. The energy production is also relatively low for the shortest wave period. In this case the plate moves very little, but the intervals where the controllable valve is closed are short, and this is when energy can be absorbed. These intervals are short because the natural period of the buoy is approximately 2.5 s, which is only slightly shorter than the period of the wave.

Table 4 shows the mean power lost in the hydraulic system, P_l. The losses in the hydraulic system is, in this model, associated with the turbulent flow through the valves. When the controllable valve is opened, there is usually a pressure difference across it, and some oil will flow through the valve to equalise the pressure. The associated energy loss seems to be much larger than the loss associated with the flow after the pressures have become almost equal, and there is a more continuous flow through the valve. This latter part of the loss is present for all valves, and will depend on the diameters of the valves, which in this case have been 0.1 m for all the valves. The diameter of the operable valve is most significant, since the flow through this valve is much larger than the flow through the other valves. If the diameter of this valve is reduced, the damping loss of the motion increases, and the excursion of the buoy is reduced. From the results in table 4 we observe that the power loss is largest for the short wave periods, and for wave periods 5 s and longer this loss is not very significant. These results indicate that the diameter of the valves used in the present calculation is large enough, and that the diameter of the check valves could probably be reduced.

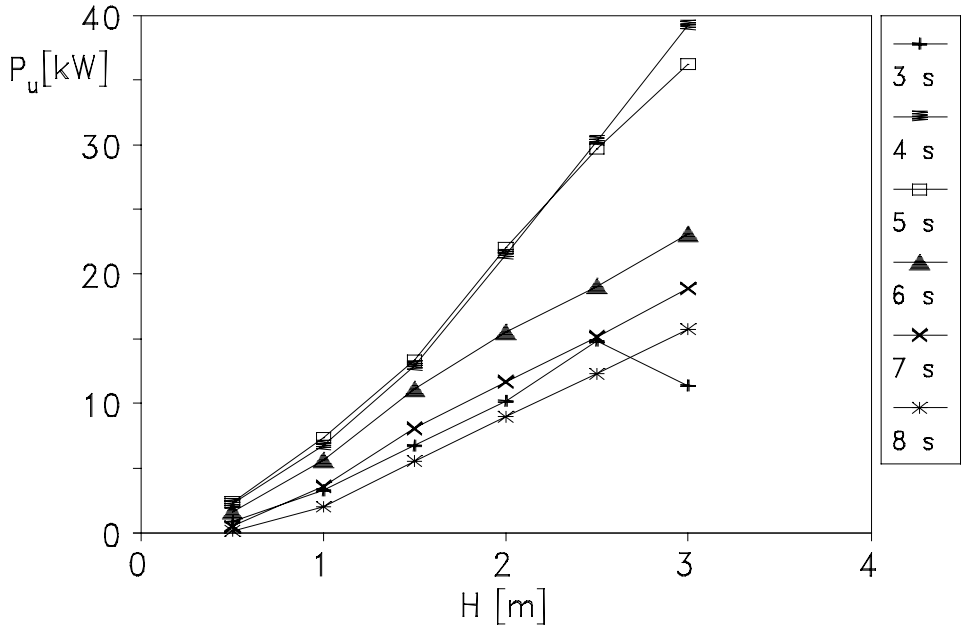

Figure 5. *Mean power production in sinusoidal waves, as function of the wave height, for different wave periods.*

T [s]	H [m]					
	0.5	1.0	1.5	2	2.5	3.0
3	0.9	3.3	6.7	10.2	14.8	11.4
4	2.2	6.7	12.9	21.5	30.3	39.2
5	2.4	7.3	13.3	22.0	29.7	36.2
6	1.6	5.6	11.1	15.5	19.0	23.1
7	0.5	3.6	8.1	11.7	15.1	18.9
8	0.1	2.0	5.5	9.0	12.3	15.7
9	0.0	0.9	3.8	7.0	9.8	14.0

Table 3. *Mean power production in sinusoidal waves, P_u [kW].*

The mean power dissipated due to the non-linear drag force, P_{drag}, is shown in table 5. The energy dissipation does in general increase with the wave period. Due to the large mass and added mass of the plate it moves more for long wave periods than for shorter wave periods, and thus the energy dissipation increases with the wave period. Further, P_{drag} increases with the wave height for small wave heights, but for most wave periods it decreases again for the largest wave heights. This is probably due to the control strategy involved in the calculations. The choice of drag coefficient C_D, which in this case has been 10, influences the calculation results significantly. However, it is very difficult to determine the appropriate drag coefficient, and the literature contains little information about drag coefficients for plates in oscillatory flow. With a smaller drag coefficient the excursion of the plate will increase, and with a larger drag coefficient the excursion of the plate will be reduced. In the limits $C_D = 0$ and $C_D \to \infty$ the power dissipated by the drag force is zero, and somewhere between the dissipated power has a maximum. If $C_D \to \infty$ the system will behave as a tight-moored device, since the plate will not move very much.

The most extreme excursion of the piston relative to the cylinder, in positive and negative direction (s_{max} and s_{min}), over the wave cycle is shown in table 6. Since the cylinder is connected to the buoy and the piston is connected to the plate, this corresponds to the excursion of the plate relative to the buoy. Ideally, the excursion of the piston should not be larger than ± 2.0 m, because the end-stop device should not be engaged. The control strategy described in Appendix D has been developed so that the energy production should be as large as possible, while the end-stop device should not be engaged on a regular basis. However, this control strategy is not equally efficient for all wave periods. In addition, the buoy should not become totally submerged, because the calculation results are then not expected to be correct. For the shortest wave period the excursion exceeds the design limit for wave height 1.5 m and larger. However, these wave conditions are not very likely to occur, so nothing has been done to improve the control procedure for these wave conditions. For longer wave periods the mean position of the piston (and plate) tends to be negative, and the excursion is significantly below the design limit. These are wave conditions where the opening instant of the controllable valve has been delayed relatively much relative to the optimum unconstrained opening instant. A better control procedure should be able to keep the plate closer to the desired mean position, and it should be possible to increase the energy absorption by increasing the excursion.

The mean flow through the hydraulic motor is shown in table 7, and maximum and minimum cylinder pressure over the wave cycle is shown in table 8. We note that the flow through the motor and the pressures in the cylinder are within the limits described in Appendix B. If the initial pressure difference between the accumulators had been chosen to be larger, the forces working between the two bodies would have been larger, in order to achieve larger energy production. This would result in larger excursion for the plate, and more power dissipated by the non-linear drag force. It will probably be necessary to know the wave climate at the location of the WEC to determine the best possible dimensions for the hydraulic system.

T [s]	*H* [m]					
	0.5	1.0	1.5	2	2.5	3.0
3	0.3	0.7	1.4	2.3	3.7	1.7
4	0.2	0.4	0.7	1.1	1.7	2.0
5	0.1	0.3	0.5	0.8	0.8	1.0
6	0.1	0.2	0.3	0.3	0.3	0.3
7	0.1	0.1	0.2	0.0	0.1	0.1
8	0.0	0.1	0.1	0.1	0.1	0.1
9	0.0	0.0	0.0	0.0	0.1	0.0

Table 4. *Mean power lost in the hydraulic machinery (valves) in sinusoidal waves, P_l [kW].*

T [s]	*H* [m]					
	0.5	1.0	1.5	2	2.5	3.0
3	0.0	0.1	0.2	0.3	0.4	0.2
4	0.2	0.4	0.9	1.8	3.2	4.0
5	0.9	1.6	3.0	3.7	2.7	2.4
6	1.7	3.0	5.0	2.4	1.7	1.4
7	2.6	4.2	5.6	3.1	2.5	2.3
8	2.4	4.9	6.2	3.7	3.5	3.4
9	1.9	5.3	7.0	4.7	4.1	5.3

Table 5. *Power dissipated by the non-linear drag force, in sinusoidal waves, P_{drag} [kW].*

T [s]	*H* [m]					
	0.5	1.0	1.5	2	2.5	3.0
3	0.33 -0.94	0.48 -1.54	0.70 -2.16	1.07 -2.16	1.66 -2.18	0.75 -2.65
4	0.05 -1.20	-0.21 -2.01	0.22 -2.11	1.08 -1.94	1.84 -1.99	2.05 -2.25
5	-0.01 -1.24	-0.17 -2.05	0.73 -1.92	1.69 -1.03	0.84 -1.67	0.83 -1.73
6	0.02 -1.03	-0.28 -1.74	0.44 -1.64	-0.20 -1.68	-0.38 -1.76	-0.49 -1.78
7	0.08 -0.76	-0.20 -1.45	1.64 0.10	-0.53 -1.62	-0.68 -1.71	-0.69 -1.86
8	0.09 -0.43	-0.14 -1.03	1.56 0.26	-0.69 -1.57	-0.72 -1.59	-1.13 -1.95
9	0.02 -0.30	-0.02 -0.72	1.23 0.25	-0.45 -1.25	-1.08 -1.71	-0.83 -1.70

Table 6. *Extreme excursion of the piston, in positive and negative direction (s_{min} and s_{max} [m]), over the wave cycle, in sinusoidal waves.*

T [s]	*H* [m]					
	0.5	1.0	1.5	2	2.5	3.0
3	0.14	0.46	0.81	1.09	1.41	1.32
4	0.33	0.86	1.39	1.98	2.45	3.12
5	0.37	0.92	1.39	1.94	2.40	2.73
6	0.25	0.75	1.22	1.58	1.83	2.09
7	0.09	0.53	0.92	1.31	1.57	1.85
8	0.01	0.31	0.69	1.09	1.37	1.63
9	0.00	0.14	0.51	0.90	1.16	1.51

Table 7. *Mean flow through the hydraulic motor in sinusoidal waves, Q_m [10^{-3} m^3/s].*

T [s]	H [m]					
	0.5	1.0	1.5	2	2.5	3.0
3	13.2 6.9	13.5 6.3	14.0 5.5	14.3 4.8	14.8 4.1	15.0 5.2
4	13.4 6.7	14.0 6.0	14.8 5.1	15.6 4.2	16.5 3.3	17.8 4.2
5	13.4 6.7	14.2 5.9	14.9 4.7	15.6 3.7	16.3 3.4	16.9 3.1
6	13.3 6.8	13.9 6.2	14.5 5.1	15.0 4.9	15.4 4.6	15.8 4.3
7	13.1 7.1	13.6 6.6	14.1 5.1	14.7 5.3	15.1 5.0	15.5 4.6
8	13.0 7.0	13.4 6.8	13.9 5.5	14.4 5.7	14.8 5.3	15.2 4.9
9	13.0 7.0	13.2 7.0	13.6 6.0	14.2 5.9	14.5 5.6	15.0 5.1

Table 8. *Maximum and minimum cylinder pressure, p_{max} and p_{min} [MPa], over the wave cycle, in sinusoidal waves.*

4.2 Irregular waves

For simulations in irregular waves a Pierson-Moskowitz (PM) spectrum[24] with wind speed as parameter is used. This spectrum is supposed to describe a fully developed sea-state. The zero-upcross period increases linearly with the wind speed and the significant wave height has a quadratic increase with the wind speed. Time series are generated for the wave elevation, which are composed of 100 components of regular waves with frequencies from 0.01 to 1.0 Hz, with $\Delta f = 0.01$ Hz. The amplitudes of the wave components are obtained from the spectrum, and the phases are selected by random choice. The wave series repeats itself after 100 s, due to the choice of Δf.

The total length of the calculated time series have been 300 s, which is three times the repeating time of the wave series. The first 200 s were not used, as this time interval was expected to include transient motions. Separate calculations were carried out to confirm that the last 100 s represented a periodic solution (with period 100 s). The control procedure used in the calculations is the same as used for sinusoidal waves, and it is described in Appendix D. Note that due to the control strategy involved, we cannot expect the solution to be exactly, but approximately, the same in each 100 s period.

	Wind speed U [m/s]										
	5	6	7	8	9	10	11	12	13	14	15
H_s [m]	0.5	0.7	0.9	1.3	1.6	2.0	2.4	2.9	3.4	4.0	4.6
T_z [s]	2.7	3.3	3.8	4.3	4.9	5.3	5.9	6.4	6.9	7.4	7.9
P_u [kW]	0.4	1.4	2.5	3.8	5.3	6.6	7.7	9.2	11.2	12.7	14.9
P_l [kW]	0.1	0.1	0.1	0.2	0.2	0.2	0.1	0.1	0.1	0.1	0.1
P_{drag} [kW]	0.3	0.6	1.1	1.9	2.7	3.2	3.6	4.1	4.9	6.0	6.7
s_{max} [m]	0.57	0.38	0.40	0.53	0.71	0.67	0.96	0.77	0.79	0.81	0.88
s_{min} [m]	-1.02	-1.40	-1.67	-1.90	-1.99	-2.07	-2.06	-2.29	-2.33	-2.26	-2.43
p_{max} [MPa]	13.1	13.4	13.7	13.9	14.2	14.5	14.7	15.0	15.2	15.6	16.1
p_{min} [MPa]	6.9	6.7	6.3	5.9	5.5	5.3	4.9	4.7	4.5	4.1	3.9
Q_{max} [10^{-3} m^3/s]	0.10	0.35	0.61	0.83	1.09	1.27	1.45	1.68	1.87	2.11	2.42
Q_m [10^{-3} m^3/s]	0.06	0.23	0.37	0.54	0.71	0.84	0.93	1.07	1.25	1.37	1.52

Table 9. *Results from simulations in irregular waves. The results shown are the mean values of ten simulations for each wind speed.*

The results from the calculations are summarised in table 9. Each entry in the table is the mean value of ten calculations performed for the same wind speed, but with different random phases. The table also includes estimates for significant wave height, H_s, and zero-upcross period, T_z. We note that the truncation of the spectrum means that H_s is slightly smaller and T_z slightly larger than for the non-truncated PM-spectrum.

Figure 6 shows the mean power production, P_u, as function of the significant wave height. The energy production has an almost linear increase with the significant wave height. It has previously been shown that for a tight-moored device with control it is possible to obtain a very rapid increase in the energy production with the significant wave height, for small wave heights, while for larger waves the increase is slower.[25] However, it has not been possible to obtain this rapid increase from the slack-moored device. Table 9 also includes the mean power dissipated due to the non-linear drag force, which is approximately 50% of the power production. This loss is significantly larger than the loss in the hydraulic machinery, P_l. The sum of the power production and the power dissipated due to the non-linear drag force for the slack-moored device is close to the power production of the tight-moored device for large wave heights, but significantly below for smaller wave heights.

The absolute value of the most extreme excursion of the piston relative to the cylinder is shown as function of the significant wave height in figure 7. Note that each entry in the

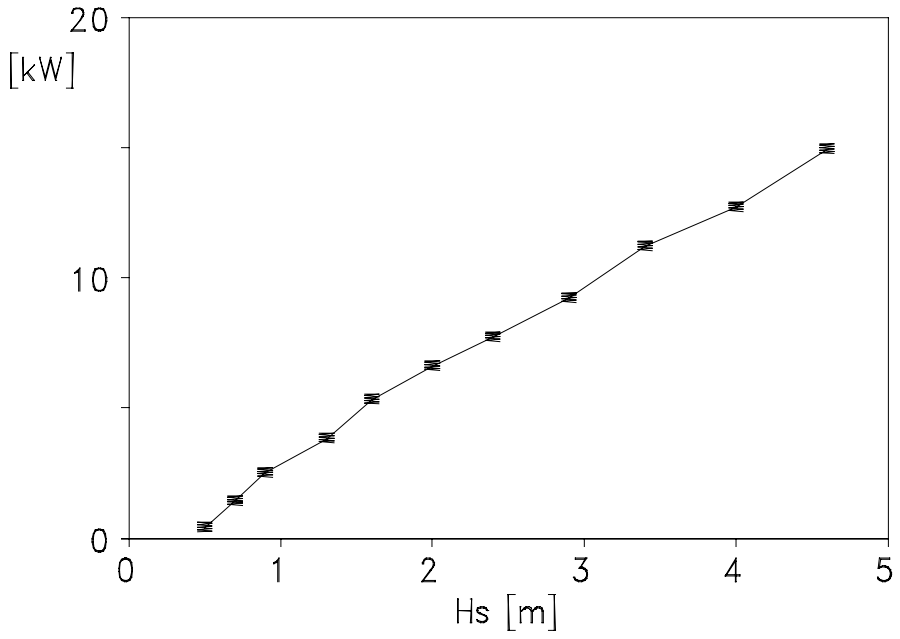

Figure 6. *Mean power produced in irregular waves, as function of significant wave height.*

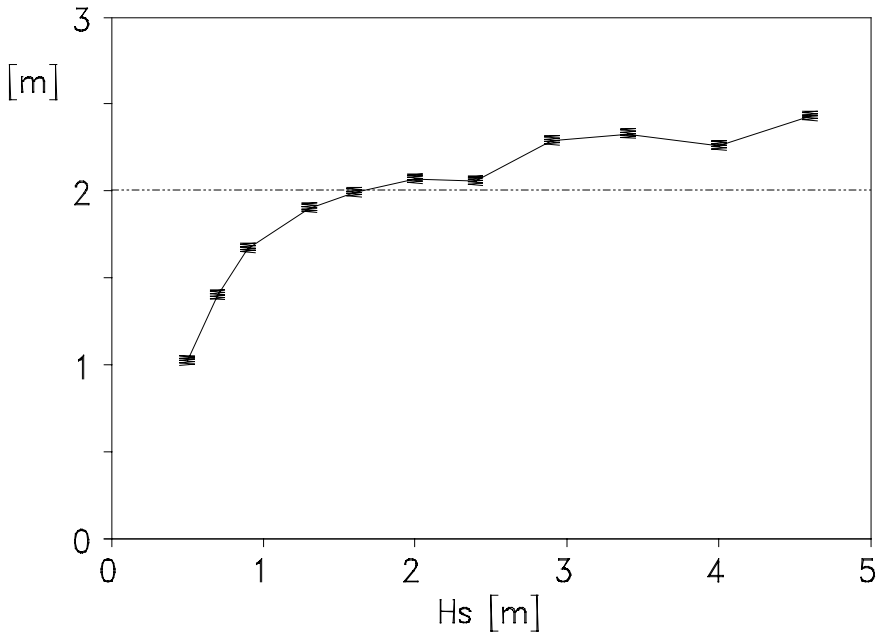

Figure 7. *Absolute value of the most extreme excursion of the piston relative to the cylinder in irregular waves, as function of significant wave height.*

figure is the mean value of the results from ten calculations, where the significant wave height is the same, but the random phases are different. The most extreme excursion is always in the negative direction. Further, for significant wave height larger than 2 m the excursion exceeds the design limit, which is not desirable. This indicates that the control procedure should be improved so that the excursion is more symmetric around the equilibrium, and that it should be more efficient in constraining the excursion in the largest waves, so that the excursion exceeds the design limit less frequently. The results also show that the end-stop device should have been more efficient, because in several instances the excursion of the piston exceeds the envisaged length of the cylinder. Note that this does not make the calculation results incorrect, since the length of the hydraulic cylinder does not enter into the mathematical model.

4.3 Year-average power production

In order to determine the year-average power production a JONSWAP-spectrum[26] is chosen as a basis for generating irregular waves. As input parameters to the spectrum are chosen the significant wave height, H_s, and the zero-upcross period, T_z.[12,27] In addition the peakedness of the spectrum is taken to be 3.3. Time series for the wave elevations are generated, which are composed of 250 components of regular waves with frequencies from 0.01 to 2.5 Hz, with $\Delta f = 0.01$ Hz. The amplitudes of the wave components are obtained from the spectrum, and the phases are selected by random choice. The wave series repeats itself after 100 s, due to the choice of Δf.

The total length of the calculated time series, for each sea state, has been 300 s, which is three times the repeating time of the wave series. For computation of the converted power the first 200 s were not used, since we want to make sure that a stable periodic solution, free of transients, has been obtained. The 100 s period used represents one period of a periodic solution with period 100 s.

Calculations have been carried out for most of the sea states in a scatter diagram (probabilities for 84 different combinations of significant wave height and zero-upcross period) from "Haltenbanken" (64° 10.5’ N, 9° 10.0’ E) off the Norwegian coast.[28] This scatter diagram is based on observations from the years 1974 to 1978, and the average incident wave power per unit width is approximately 37 kW/m.[29] Table 10 shows the probability for each sea state in percent, table 11 shows the mean power production for each sea state and table 12 shows the mean power dissipated by the non-linear drag force for each sea state. In these calculations energy losses in the hydraulic motor have been neglected. No calculations have been performed for sea states with significant wave height larger than 6.5 m, since the buoy might then be totally submerged during parts of the series, and the computed results would not be correct. However, this accounts for only approximately 1% of the observations. For these sea states the mean power production and the power dissipated by the non-linear drag force have both been assumed to be zero.

To obtain an estimate for the year-average power production of the WEC a summation has been carried out over all sea states of the probability of the sea state multiplied by the mean power production in the sea state, and the results was 4.9 kW. By doing he same for the power dissipated due to the non-linear drag force, a year-average value of 3.8 kW was obtained.

H_s [m]	T_z [s]									
	4	5	6	7	8	9	10	11	12	13
0.5										
1.0	0.24	3.02	3.47	3.47	1.72	0.39	0.37	0.07		
1.5	0.09	4.79	6.73	5.18	3.71	2.01	0.31	0.13	0.04	
2.0		1.53	6.71	5.24	4.24	1.88	0.61	0.20	0.06	
2.5		0.15	3.12	5.09	3.39	1.75	0.68	0.35	0.11	
3.0			0.77	4.13	2.84	2.07	0.85	0.15		
3.5			0.07	1.36	2.49	1.68	0.61	0.18	0.13	
4.0				0.35	1.75	1.01	0.65	0.17		
4.5				0.06	0.90	1.25	0.42	0.22	0.02	0.02
5.0					0.17	0.76	0.33	0.09		
5.5					0.06	0.44	0.41	0.11		
6.0						0.33	0.44	0.18	0.04	
6.5						0.07	0.44	0.07	0.06	

Table 10. *Scatter table from "Haltenbanken" (64° 10.5' N, 9° 10.0' E).[28] Probability of each sea state in percent. Sea states with significant wave height larger than 6.5 m have a total probability of 1.02%.*

H_s [m]	T_z [s]									
	4	5	6	7	8	9	10	11	12	13
0.5	0.76	0.56	0.12	0.03	0.02	0.00	0.00	0.00	0.00	
1.0	2.93	2.25	1.22	0.60	0.51	0.18	0.01	0.01	0.00	
1.5	5.33	4.87	3.34	2.44	1.139	0.91	0.40	0.19	0.15	
2.0		5.95	4.69	3.93	2.78	1.82	1.64	1.45	0.69	
2.5		9.89	8.06	5.37	3.78	4.05	2.70	1.85	1.66	
3.0			9.84	6.21	5.83	4.44	4.64	3.58		
3.5			12.85	10.91	8.99	7.13	5.41	4.67	4.18	
4.0				11.92	9.66	9.21	7.36	5.76		
4.5				14.83	15.32	12.23	8.78	8.08	6.53	6.22
5.0					16.45	15.28	12.10	10.17		
5.5					19.62	16.93	13.84	12.84		
6.0						20.05	17.80	12.92	13.07	
6.5						24.20	21.63	18.97	14.13	

Table 11. *Mean power production for each sea state, when 100% efficiency has been assumed for the hydraulic motor. No calculations have been carried out for waves with H_s above 6.5 m.*

H_s [m]	T_z [s]									
	4	5	6	7	8	9	10	11	12	13
0.5	0.62	1.00	1.14	0.95	0.85	0.57	0.47	0.35	0.23	
1.0	1.23	1.99	2.61	2.60	1.89	1.73	1.76	1.54	1.26	
1.5	1.64	2.41	2.13	3.63	2.47	3.44	3.86	2.96	2.55	
2.0		2.75	2.21	4.02	4.75	4.07	4.05	3.58	4.01	
2.5		4.13	4.53	4.03	4.10	3.91	4.22	4.38	4.22	
3.0			2.82	4.08	4.95	5.04	5.36	5.57		
3.5			4.29	4.34	4.59	4.28	5.19	4.97	6.14	
4.0				5.17	5.54	5.75	6.74	6.62		
4.5				7.52	7.37	6.26	6.38	7.92	7.18	8.30
5.0					7.01	8.15	8.56	9.21		
5.5					9.62	8.14	9.59	11.74		
6.0						10.81	9.66	12.07	12.55	
6.5						9.88	11.31	11.13	11.60	

Table 12. *Power dissipated due to the non-linear drag force, for each sea state. No calculations have been carried out for waves with H_s above 6.5 m.*

Figure 8 shows a duration curve for the mean power production. This curve shows the percentage of the year for which the mean power production is above a certain value. The time resolution is three hours, the time period between the measurements of the sea state. It has previously been shown that for a tight-moored device the power output is smoother for a device with control than for a device without control.[25] That is, the power output is close to the year-average a large fraction of the year, and the full capacity of the hydraulic machinery can be utilised most of the time. The results from the present calculation is not as smooth as for the tight-moored device with control, but somewhat smoother than the output from the tight-moored device without control.

Table 13 shows some additional results, for each of the sea states. The table contains results for the mean power production, the power dissipated by the non-linear drag force, the extreme excursion of the piston relative to the cylinder in positive and negative direction, maximum and minimum cylinder pressure and maximum flow through the hydraulic motor. Maybe the most interesting result is the extreme excursion of the piston. As for the calculations carried out for the irregular waves based on the PM-spectrum, the piston has a negative mean position for most sea states, and for large waves the excursion exceeds the design limit, that is the end-stop device is engaged.

It should also be noted that the WEC is rather small for this wave climate, and for a larger buoy, with a longer hydraulic cylinder, it will probably be easier to keep the excursion within the design limit.

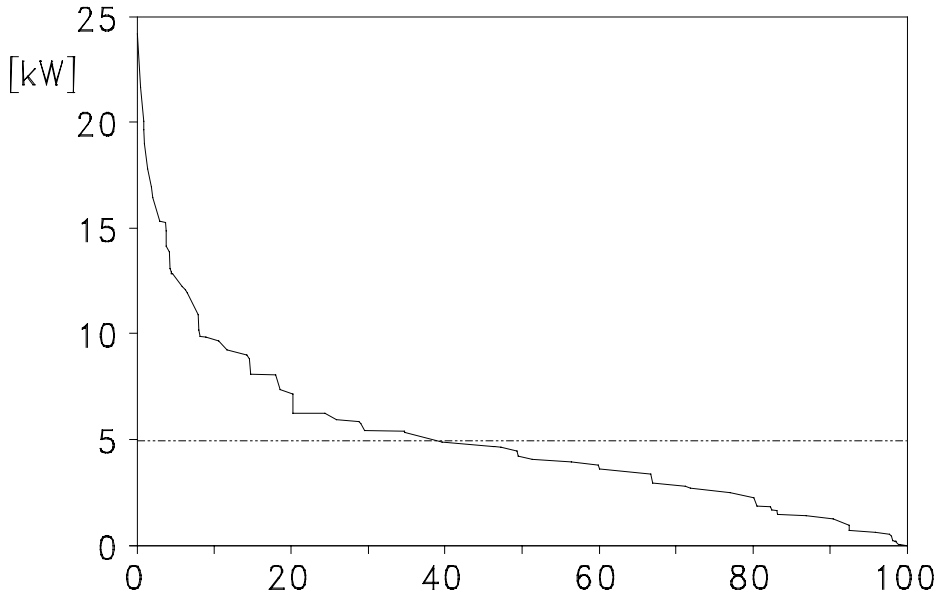

***Figure 8**. Duration curve for the mean power production, giving the percentage of the year the mean power production is above a certain level. The horizontal line is the year-average.*

5 Conclusion

A mathematical model is presented for a slack-moored wave-energy converter, consisting of a semi-submerged heaving buoy moving relative to a submerged plate. The geometry is chosen so that the heave excitation forces on the two bodies are approximately equal in magnitude, but in opposite direction, for wave periods we want to absorb energy from. A high-pressure hydraulic machinery is proposed for energy production and motion control. The model is based on linear hydrodynamic theory, but the forces from the end-stop device and the hydraulic system are non-linear. In addition a non-linear drag force is included on the plate. The buoy is, in general, exposed to an irregular incident wave, and oscillations in heave only are considered. The numerical model has been compared to an analytical solution for a somewhat simplified system, and good agreement is observed between the numerical and analytical solution. However, when the buoy becomes fully submerged the numerical model is not expected to give correct results.

A procedure has been presented for control of the device in both sinusoidal and irregular waves. This procedure determines the opening instant of the controllable valve so that, in small waves the extrema of the relative velocity between the bodies coincide with the extrema of the excitation force, while in larger waves the opening instant is delayed to constrain the excursion. The control procedure is also used to keep the plate in the desire equilibrium position, since the submerged body has no hydrostatic stiffness.

Table 13. *Results from simulations in irregular waves. The following parameters are given; zero-upcross period (T_z [m]), significant wave height (H_s [m]), extreme excursion of piston in positive and negative direction (s_{max} [m] and s_{min} [m]), maximum and minimum cylinder pressure (p_{max} [MPa] and p_{min} [MPa]), maximum flow through hydraulic motor (Q_{max} [10^{-3} m^3/s]), mean power production (P_u [kW]) and mean power dissipated due to the non-linear drag force (P_{drag} [kW]).*

T_z	H_s	s_{max}	s_{min}	p_{max}	p_{min}	Q_{max}	P_u	P_{drag}
4.0	0.5	0.40	-0.98	13.2	6.9	0.17	0.76	0.62
5.0	0.5	0.25	-1.02	13.2	7.0	0.16	0.56	1.00
6.0	0.5	0.69	-0.82	13.1	6.7	0.05	0.12	1.14
7.0	0.5	0.42	-0.75	13.0	7.0	0.01	0.03	0.95
8.0	0.5	0.31	-0.69	13.0	7.1	0.01	0.02	0.85
9.0	0.5	0.22	-0.45	13.0	7.0	0.00	0.00	0.57
10.0	0.5	0.19	-0.50	13.0	7.8	0.00	0.00	0.47
11.0	0.5	0.13	-0.35	13.0	7.5	0.00	0.00	0.35
12.0	0.5	0.09	-0.26	12.6	8.0	0.00	0.00	0.23
4.0	1.0	0.27	-1.62	13.8	6.1	0.71	2.93	1.23
5.0	1.0	0.47	-1.73	13.6	6.2	0.52	2.25	1.99
6.0	1.0	0.45	-1.26	13.3	6.8	0.32	1.22	2.61
7.0	1.0	1.19	-0.73	13.2	6.5	0.22	0.60	2.60
8.0	1.0	0.34	-1.02	13.2	7.2	0.23	0.51	1.89
9.0	1.0	-0.29	-1.46	13.1	7.5	0.09	0.18	1.73
10.0	1.0	0.67	-0.29	13.0	6.8	0.00	0.01	1.76
11.0	1.0	0.47	-0.53	13.0	7.0	0.00	0.01	1.54
12.0	1.0	0.22	-0.37	13.0	7.0	0.00	0.00	1.26
4.0	1.5	0.45	-2.27	14.2	5.6	1.05	5.33	1.64
5.0	1.5	0.47	-1.73	14.1	5.8	0.98	4.87	2.41
6.0	1.5	0.16	-2.19	14.0	5.6	0.91	3.34	2.13
7.0	1.5	0.49	-1.55	13.6	6.3	0.58	2.44	3.63
8.0	1.5	0.02	-2.06	13.8	6.6	0.73	1.39	2.47
9.0	1.5	0.56	-1.17	13.4	6.8	0.36	0.91	3.44
10.0	1.5	0.95	-0.85	13.2	6.4	0.14	0.40	3.86
11.0	1.5	0.97	-0.49	13.1	6.4	0.09	0.19	2.96
12.0	1.5	0.69	-0.94	13.1	6.7	0.07	0.15	2.55
5.0	2.0	0.42	-2.09	14.4	5.6	1.20	5.94	2.75
6.0	2.0	0.03	-1.80	14.6	5.5	1.37	4.69	2.21
7.0	2.0	0.39	-2.01	14.0	5.9	0.92	3.93	4.02
8.0	2.0	0.48	-1.57	13.8	6.1	0.72	2.78	4.75
9.0	2.0	0.66	-1.39	13.6	5.8	0.52	1.82	4.07
10.0	2.0	0.41	-2.24	13.6	6.6	0.51	1.64	4.05
11.0	2.0	-0.44	-1.87	13.7	7.1	0.63	1.45	3.58
12.0	2.0	0.55	-0.91	13.2	6.8	0.23	0.69	4.01
5.0	2.5	0.98	-2.32	15.1	4.7	1.74	9.89	4.14
6.0	2.5	0.55	-1.70	14.6	5.1	1.41	8.06	4.53
7.0	2.5	0.31	-2.11	14.3	5.2	1.11	5.37	4.03

8.0	2.5	0.21	-2.25	14.3	5.2	1.11	3.78	4.10
9.0	2.5	0.22	-2.10	14.2	6.3	1.06	4.05	3.91
10.0	2.5	0.10	-2.01	13.9	5.8	0.77	2.70	4.22
11.0	2.5	0.56	-1.29	13.9	6.3	0.78	1.85	4.38
12.0	2.5	0.02	-2.21	13.9	6.8	0.78	1.66	4.22
6.0	3.0	-0.01	-2.51	15.0	4.8	1.71	9.84	2.82
7.0	3.0	-0.06	-2.50	15.2	4.9	1.84	6.20	4.08
8.0	3.0	0.49	-2.11	14.4	5.3	1.24	5.83	4.95
9.0	3.0	0.26	-2.43	14.4	5.9	1.22	4.44	5.04
10.0	3.0	1.18	-1.82	14.2	5.7	1.08	4.64	5.36
11.0	3.0	0.85	-0.90	13.9	5.4	0.80	3.58	5.57
6.0	3.5	0.90	-2.04	15.2	4.5	1.86	12.85	4.29
7.0	3.5	0.47	-2.14	15.2	4.6	1.86	10.91	4.34
8.0	3.5	0.01	-2.36	14.9	4.5	1.58	8.99	4.59
9.0	3.5	-0.27	-2.18	15.0	5.6	1.71	7.13	4.28
10.0	3.5	-0.04	-2.48	14.7	6.2	1.45	5.41	5.19
11.0	3.5	0.86	-2.21	14.7	5.0	1.45	4.67	4.97
12.0	3.5	-0.11	-1.64	14.2	5.3	1.05	4.18	6.14
7.0	4.0	1.30	-2.56	16.3	4.2	2.62	11.92	5.17
8.0	4.0	0.26	-2.73	15.4	4.7	1.94	9.66	5.54
9.0	4.0	0.99	-2.45	15.4	4.5	1.93	9.21	5.75
10.0	4.0	-0.09	-2.21	15.1	5.0	1.78	7.36	6.74
11.0	4.0	0.15	-2.33	14.9	5.7	1.62	5.76	6.62
7.0	4.5	1.26	-2.43	16.9	3.4	2.94	14.83	7.53
8.0	4.5	1.55	-2.33	15.9	3.8	2.32	15.32	7.37
9.0	4.5	0.00	-2.35	15.6	4.1	2.11	12.23	6.26
10.0	4.5	0.27	-2.35	15.5	5.2	2.06	8.78	6.38
11.0	4.5	0.05	-2.63	14.7	4.7	1.45	8.08	7.92
12.0	4.5	0.89	-2.28	14.5	4.7	1.34	6.53	7.18
13.0	4.5	0.99	-2.17	14.9	5.1	1.64	6.22	8.30
8.0	5.0	1.46	-1.85	16.3	4.0	2.57	16.45	7.01
9.0	5.0	0.52	-2.46	16.3	3.9	2.60	15.28	8.15
10.0	5.0	0.51	-2.14	15.8	4.1	2.26	12.10	8.56
11.0	5.0	0.00	-2.66	15.3	4.5	1.89	10.17	9.21
8.0	5.5	1.36	-2.49	17.1	3.0	3.06	19.62	9.62
9.0	5.5	0.62	-2.30	15.9	3.9	2.33	16.93	8.14
10.0	5.5	0.61	-2.68	15.8	4.1	2.23	13.84	9.59
11.0	5.5	0.78	-2.48	15.9	3.8	2.33	12.84	11.74
9.0	6.0	1.61	-2.26	16.9	3.2	2.96	20.05	10.81
10.0	6.0	0.02	-2.42	16.7	3.9	2.83	17.80	9.66
11.0	6.0	-0.35	-2.96	15.7	4.2	2.20	12.92	12.07
12.0	6.0	1.16	-2.18	15.7	4.5	2.16	13.07	12.55
9.0	6.5	0.62	-2.57	16.9	3.7	2.99	24.20	9.88
10.0	6.5	2.16	-2.42	17.7	3.0	3.41	21.63	11.31
11.0	6.5	2.34	-2.21	17.9	3.2	3.51	18.97	11.13
12.0	6.5	0.87	-2.92	16.4	3.3	2.66	14.13	11.60

Results are presented for calculations in sinusoidal waves and irregular waves based on a Pierson-Moskowitz spectrum. In sinusoidal waves the energy production is largest in waves with period 4 s and 5 s. The control procedure is not totally successful, since the mean position of the piston is usually negative for long wave periods, and the full length of the available piston stroke is not utilised. In irregular waves the power production has an approximately linear increase with the significant wave height. The control procedure is not able to constrain the excursion sufficiently, so the end-stop device is engaged too often. The excursion of the piston does also here usually have a negative mean value, which means that the available piston stoke is not fully utilised. By further development of the control procedure it should be possible to solve these problems, and at the same time increase the power production.

It has been found that one of the most important forces on the plate is the non-linear drag force, and it is also responsible for dissipation of a relatively large fraction of the power absorbed from the incident wave. Relatively little is known about the drag force, especially for plates in oscillatory flow, and in the presents calculations a relatively simple model has been used. More understanding of the drag force will be important for the development of this kind of WEC.

On the basis of a scatter table, for a wave climate where the average incident wave power per unit width is approximately 37 kW/m, the year-average power production is estimated to be approximately 4.9 kW. Further, a duration curve is presented, which shows the percentage of the year the mean power production is above a certain level. The power production should be close to the year average a large fraction of the year, so that the power output is smooth. The power output from the slack-moored device is not as smooth as the power output from a tight-moored device with control, which has previously been investigated, but more smooth than the power output from a tight-moored device without control. It is estimated the power dissipated by the non-linear drag force on the plate has a year average value of 3.8 kW. It should be noted that the WEC investigated is small for the wave climate used in this calculation.

The design of the hydraulic system proposed for the present WEC is similar to the hydraulic system used in a tight-moored WEC previously studied. For the tight-moored device the hydraulic system worked satisfactory, and the output power increased very rapidly with the wave height for small wave heights. It has not been possible to obtain the same rapid increase for the present slack-moored device. It has also turned out that keeping the submerged plate in the desired mean position is a problem, as is constraining the excursion in large waves. Further research should be carried out to determine if a different machinery could increase the power production, and at the same time be easier to control. The problems encountered with the present WEC design is that the power dissipated by the non-linear drag force is large, and we are not able to produce the same rapid increase in the power production for small wave heights as with a tight-moored WEC. It should be investigated if changing the geometry of the bodies could lead to increased energy production. In the present calculations the hydrodynamic parameters for the device have only been rough approximations, and a model should be developed to determine the parameters for this kind of geometry.

Acknowledgements

The author wishes to thank Per Magne Lillebekken and Professor Johannes Falnes for stimulating discussions and valuable comments during the work.

Appendix A. A geometry with force compensation

We consider a geometry consisting of a floating cylindrical buoy and a concentric submerged plate. The geometry of the bodies should be chosen so that the excitation force on the two bodies are approximately equal in magnitude, but in opposite direction, for the wave periods we want to absorb energy from.[1] A mathematical model has been developed for computing the hydrodynamic parameters for a system of two vertical concentric cylinders of the same radius, where one cylinder is semi-submerged while the other is submerged.[19] When the height of the submerged cylinder is small, it represents a floating plate with sharp edges. However, the program cannot handle a geometry where the buoy and plate have different radii. This means we have to make some approximations. We make two calculations, one where the radius of both bodies is equal to the envisaged radius of the buoy, and we adopt the excitation force coefficient ($\hat{f}_{e,b}$) and the radiation resistance (R_{11}) for the buoy from this calculation. In the other calculation the radius of both bodies is equal of the envisaged radius of the plate, and we adopt the excitation force coefficient ($\hat{f}_{e,p}$) and the radiation resistance (R_{22}) for the plate from this calculation. The assumption is then that these hydrodynamic parameters are not significantly influenced by the radius of the other body. The off-diagonal elements of the radiation resistance matrix can be determined from the following relation[30]

$$R_{12} R_{21} = R_{11} R_{22} \tag{12}$$

We also note that $R_{12} = R_{21}$ due to the symmetry of the radiation impedance matrix. Ordinarily the excitation forces on the two bodies should be anti-phase. However, since in our case the two excitation force coefficients are taken from two different calculations, and this phase relationship is not (accurately) satisfied. The phase discrepancy is in this case approximately 5° for $\omega = 1.0$ rad/s, 45° for $\omega = 2.0$ rad/s and 115° for $\omega = 3.0$ rad/s. However, it has not been determined what influence this inaccuracy has on the validity of the computed results.

Figure 9 shows the amplitude of the excitation force coefficient for a buoy with diameter 3.3 m and draft 3.1 m, and for plates with diameter 6 m and 8 m, both with thickness 0.2 m and submergence 10 m. We observe that for the plate with diameter 6 m we do not obtain force compensation for any frequency. For the larger plate we have reasonably good force compensation for frequencies between 0.7 rad/s and 1.7 rad/s, corresponding to wave periods from 4 s to 9 s. This is approximately the frequency interval for which it is desirable to have force compensation. We note that in addition to the diameter of the plate, the submergence of the plate will also strongly influence the excitation force. The excitation

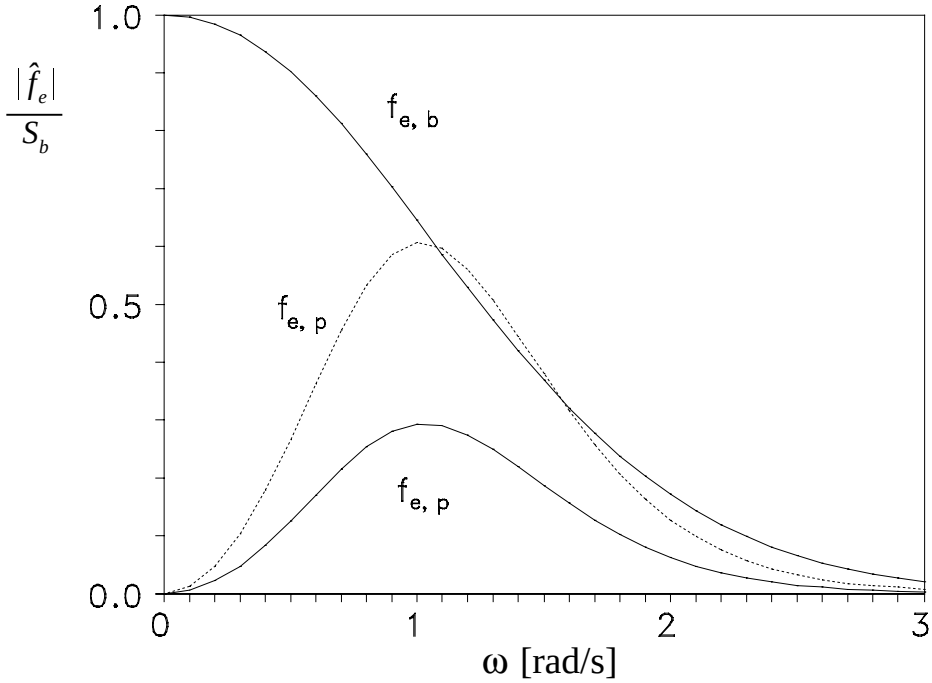

Figure 9. *Normalised excitation force coefficients, as function of the frequency, for the buoy ($f_{e,b}$) and for the plate ($f_{e,p}$). The solid line is for a plate with diameter 6 m and the dotted line is for a plate with diameter 8 m.*

force coefficients presented here have been used to determine the integration kernels shown in figure 2. Falnes has shown that for a small vertical piston, moving in surge, in a vertical wall, the excitation force kernel becomes "more non-causal" when the submergence increases.[31] That is consistent with the present observation, that the excitation kernel for the buoy tends faster to zero than the excitation force kernel for the plate. In addition, the area under the curve for the excitation force kernels should be equal to the hydrostatic stiffness for the body, which means that for the plate the area under the curve should be zero. This explains the oscillatory behaviour on the curve for $f_{e,p}(t)$.

Figure 10 shows the radiation resistances for the geometry with the large plate. We have the following reciprocity relation[32] between the elements of the radiation resistances and the excitation forces on the two bodies

$$R_{ij} = \frac{k}{8J} F_i F_j^* \tag{13}$$

where J is the wave power transport per unit wave frontage and the asterisk indicates complex conjugate. This relation explains the rough equality of R_{11}, R_{12} and R_{12} in the frequency region of force compensation. However, since the excitation force coefficients in this case have been computed by two different calculations this relation will not be exact for the cross terms. The radiation kernels shown in figure 3 are computed from the radiation

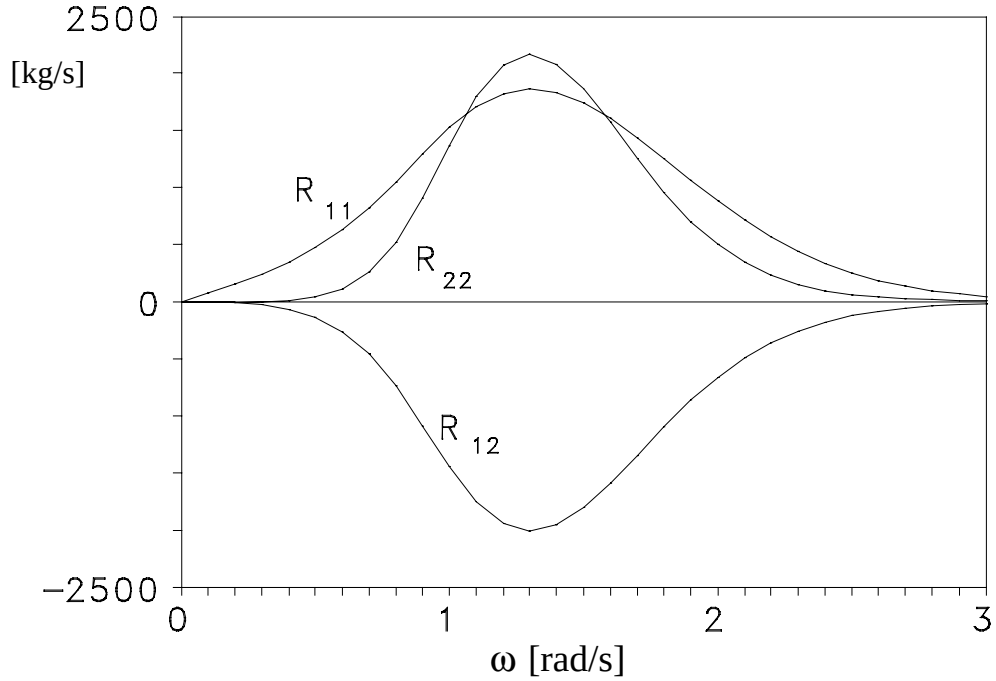

Figure 10. *Radiation resistance as function of the frequency for a buoy with diameter 3.3 m and a plate with diameter 8.0 m.*

resistances shown in figure 10. The integration kernels have zero-crossing at approximately the same instants. This is probably not a general property, but is due to the similarity between the radiation resistances for a system which has approximate force compensation.

The final parameter necessary to compute the radiation forces, given in equation (3), is the added mass matrix at infinite frequency. From the two calculations the following values are estimated $m_{r,11}(\infty) = 8700$ kg and $m_{r,22}(\infty) = 190000$ kg. It is then assumed that the added mass of one body is not significantly influenced by the radius of the other body. In this case it is no reciprocity relation which can be used to determine the cross terms $m_{r,12}(\infty) = m_{r,21}(\infty)$. From the two calculations, corresponding to the small and large diameters, the following approximations $m_{r,12}(\infty) = -2000$ kg and $m_{r,12}(\infty) = -14000$ kg are obtained, and we choose to use the mean value $m_{r,12}(\infty) = -8000$ kg.

Appendix B. The hydraulic systems

The hydraulic system discussed in the paper, as proposed by Budal,[33] is shown in figure 4. The hydraulic system can be used both for a single oscillating body, moving relative to a fixed reference, and for two oscillating bodies, where the relative motion between the bodies is used to absorb energy. This system is based on discrete control of the motion (latching), and not continuous control. How the system is supposed to control the motion of the WEC, and produce useful energy, has been described earlier.[33] Phase control is

obtained by means of an operable valve which closes or opens the connection from the cylinder to a gas accumulator (*A*) placed inside the hull of the buoy. Amplitude control is achieved through two check valves (or operable valves) between the cylinder and one high pressure gas accumulator (*B*) and one low pressure gas accumulator (*C*). We note that these valves should be open only when the controllable valve is closed, that is, when the connection from the cylinder to accumulator *A* is closed. The pressure difference between these accumulators is used to run a hydraulic motor, and produce useful energy.

There is a fourth gas accumulator (*D*), which was not included in the original proposal, connected directly to the cylinder. This accumulator is small, and is used to smoothen the pressure in the system, and to avoid pressure peaks. This is desirable, so that the components of the hydraulic machinery are not subject to very rapid changes in pressure. In the mathematical model this accumulator can also be used to simulate the compressibility of the oil in the hydraulic cylinder. The pressure in this accumulator is assumed to be equal to the pressure in the cylinder.

The pressure and volume of the gas accumulators are assumed to be related by the following formula

$$p\,V^{\gamma} = \text{constant} \tag{14}$$

When the process is adiabatic, we have $\gamma = 1.4$, and when the process is isothermal, $\gamma = 1.0$. Heat transfer has not been included in the model.

The dimensions of the hydraulic system are determined as follows. The force from the hydraulic piston-and-cylinder shall keep the two bodies in the desired equilibrium positions. The piston shall, in this case, at equilibrium, act on the buoy with a force of 173 kN downwards, which is determined by the mass of the body and the submerged volume at equilibrium, and on the plate with an equal force in the opposite direction. Assuming an equilibrium pressure of 10 MPa, it is necessary to have a net piston area $A_p = 0.0173\ \text{m}^2$. An initial pressure of 7 MPa for the low-pressure accumulator and 13 MPa for the high-pressure accumulator has been found to be suitable. The check valves to the low-pressure and high-pressure accumulators will then open when the excursion of the buoy is approximately 0.6 m from the equilibrium position, the plate is in the equilibrium position and the controllable valve is closed. During normal operation the pressure in the high-pressure accumulator should not be allowed to drop below 13 MPa, and the pressure in the low pressure accumulator should not rise above 7 MPa. However, this will depend on the control procedure used for the hydraulic motor.

The maximum displacement volume of the hydraulic motor is determined by the maximum mean flow delivered by the cylinder to the high pressure accumulator. If we assume that the piston has a maximum stroke of 4.0 m, but only delivers oil to accumulator *B* from a 1 m long part of the stroke, and assuming a wave period of 5 s, the maximum mean flow is $Q = 0.0035\ \text{m}^3/\text{s}$. If the pressure difference across the motor during operation is 10 MPa the maximum power is approximately 35 kW. This is a reasonable number for a WEC of this size. Further, when the piston moves 2.0 m out from its equilibrium position in either direction, with the controllable valve open, the check valves to accumulator *B* and *C* should not open. This means that the check valves will open only when the controllable valve is closed. Assuming that the gas in accumulator *A* can be described by the adiabatic equation (14), and that the equilibrium pressure in the accumulator is 10 MPa, the gas volume in the accumulator in the equilibrium position can be chosen to be $0.30\ \text{m}^3$. The

total volume of the accumulator can then for instance be chosen to be $0.40\,\mathrm{m}^3$.

The high pressure and low pressure accumulators should be able to store energy equal to maximum production of approximately 30 s, which is roughly $0.1\,\mathrm{m}^3$. This is a compromise between the desire to be able to smoothen the output power by being able to store energy, and the desire to keep the accumulators as small as possible, in order to keep the weight as low as possible. It is important to note that the combined oil volume of accumulator *B* and *C* should be almost constant during operation, otherwise the mean position of the plate will move away from the equilibrium position. If the pressure in accumulator *B* is allowed to rise to approximately 18 MPa when $0.1\,\mathrm{m}^3$ of oil is stored in it, the gas volume at equilibrium should be $0.52\,\mathrm{m}^3$, and the total volume of the accumulator could be $0.6\,\mathrm{m}^3$. If the gas volume of accumulator *C* at equilibrium is chosen to be $0.092\,\mathrm{m}^3$, the pressure drops to approximately 2.5 MPa when $0.1\,\mathrm{m}^3$ of oil is removed from it. The total volume of the accumulator could then be $0.2\,\mathrm{m}^3$. The cylinder is envisaged to be 5 m long, of which 0.5 m in each end is used for an end-stop device.

Regarding the choice of hydraulic motor, it has to have variable displacement volume, high efficiency and be able to work at the desired pressure and volume flow. For this purpose axial piston motors and wing motors seem most suitable. The motor recently proposed by Salter might also be suitable.[34] When a particular motor has been chosen, it might be necessary to change the specifications of the hydraulic system, so that the pressure over the motor and the liquid flow gives the best possible efficiency. In the present work, the displacement volume has been controlled so that at any instant the high pressure accumulator would be back to the initial state in 30 s if the displacement volume was kept constant, and no more oil was allowed to get into the accumulator.

In these calculations it is assumed that the flow between the gas accumulators is determined by the valves, and that the system of pipes is of minor importance. The valves are modelled as orifices, and the pressure drop (Δp) (difference between static upstream and downstream pressure) and flow (Q) are related as follows

$$Q = \mu A_o \sqrt{2\Delta p/\rho_o} \tag{15}$$

where μ is the orifice (discharge) coefficient, A_o is the orifice area and ρ_o the density of the hydraulic oil. This equation describes turbulent flow through the orifice. We consider a circular orifice with sharp edges. If the orifice area is much smaller than the area of the pipe, the discharge coefficient is $\mu = 0.611$. For low temperatures and small pressure differences, the flow through an orifice can also be laminar. However, this is not considered here. With this model of the hydraulic system, all the losses are associated with the flow through the valves and the linear friction force.

A summary of values of constants used in the calculations, are given in table 1, and initial values of variables are given in table 2. Note that the check valves and the operable valve are all assumed to have an area (A_o) of $0.0079\,\mathrm{m}^2$.

Appendix C. The end-stop device

It is sometimes necessary to include a deceleration cushion at the end of the stroke, and this function is carried out by the end-stop device. This device dissipates kinetic energy of the load gently, and reduces the possibility of mechanical damage to the cylinder. The force from the end-stop device can be composed of a spring term and a damping term, where the spring term represents storage of energy and the damping term represents dissipation of energy. The force is taken to be positive when acting on the buoy in the positive *z*-direction. We introduce the excursion and velocity of the piston relative to the cylinder, to simplify the equations

$$\begin{aligned} s_r(t) &= s_p(t) - s_b(t) \\ u_r(t) &= u_p(t) - u_b(t) \end{aligned} \tag{16}$$

The spring force term can be described by the following formula, when we envisage one spring placed in each end of the cylinder,

$$F_{spring}(t) = \begin{cases} k_-(s_r(t) - s_-) & when\ s_r(t) < s_- \\ 0 & when\ s_- < s_r(t) < s_+ \\ k_+(s_r(t) - s_+) & when\ s_r(t) > s_+ \end{cases} \tag{17}$$

where k_- and k_+ give the stiffness of the springs, and s_- is a negative constant and s_+ is a positive constant. This allows different spring stiffnesses in the two directions, and the end-stop device can start working at different excursions in positive and negative direction. This expression uses a linear spring (working only in one direction from its equilibrium position), but it should also be possible to use a nonlinear spring if that is desirable.

The damping force term can be described by the following formula

$$F_{fric}(t) = \begin{cases} -B_- u_r(t) u_r(t) & when\ s_r(t) < s_-\ and\ u_r(t) < 0 \\ 0 & when\ s_- < s_r(t) < s_+ \\ B_+ u_r(t) u_r(t) & when\ s_r(t) > s_+\ and\ u_r(t) > 0 \end{cases} \tag{18}$$

This models a piston-and-cylinder part of the end-stop device, with one cylinder in each end of the main cylinder of the WEC. When oil is forced out of these cylinders it flows through orifices. This creates a pressure in the cylinder, and thereby a force which tends to stop the motion of the WEC. The flow through the orifices has here been modelled to be turbulent. A linear term could also have been included to take into account laminar flow. However, this has not been done in the present model. It is assumed that the spring force is sufficient to reset the damping mechanism, or otherwise that the oil can flow freely back into the cylinder when the WEC starts moving in the opposite direction. The constants B_- and B_+ are determined by the design of the end-stop piston-and-cylinder.

Appendix D. Procedure for control in irregular waves

For operation of a WEC with a control facility, it is necessary to develop some sort of strategy on how to absorb as much energy as possible, and at the same time protect the machinery in large waves. In this case, this means that we need a strategy on how to operate the controllable valve. The procedure given here has the excitation force as input, but it could also have been based on the incident wave. The intention of this procedure is to have coinciding extrema of excitation force and relative velocity between the bodies when the waves are small. For larger waves the excursion is constrained by opening the controllable valve later, which means that the velocity phase is delayed. In addition the mean position of the submerged body should be kept close to its equilibrium position, so that the full piston stroke can be utilised.

The following is a description of the computer code for the applied preliminary control procedure. For each time step in the main program, a decision is made on whether the controllable valve should be open or closed during the next time step, and the procedure making this decision can be described as follows. When entering the procedure, the present time of the simulation is given by *t*. If the valve is closed, when the procedure is entered, it should be determined if it should remain closed or if it should be opened. It is assumed that the excitation force has been predicted a certain interval into the future, T_{pred}, and this force can be considered as the input to the procedure. In the present calculations $T_{pred} = 4.4$ s has been used. We assume that the time interval between the opening and closing of the valve is approximately $T_0/2$, where T_0 is the natural period of the buoy when the plate is being held fixed. In this case $T_0 = 2.2$ s has been used. We create the following function

$$I_{int}(t') = \int_{t'-T_0/4}^{t'+T_0/4} (F_{e,b}(t'') - F_{e,p}(t''))\,dt'' \qquad (19)$$

which is used to determine when the valve should be opened. This minus appears because the excitation force acting on the two bodies are in opposite direction, and we want to locate the extrema of the force acting between the bodies. To obtain coinciding value of relative velocity between the bodies and excitation force the valve should be opened $T_0/4$ before the extremum of $I_{int}(t')$. To constrain the excursion in large waves we introduce two variable parameters, I_{min} and I_{max}, so that, if for a maximum $I_{int}(t_{extr}) > I_{max}$ or for a minimum $I_{int}(t_{extr}) < I_{min}$, the opening of the valve is delayed.

Since the submerged body has no hydrostatic stiffness, the control procedure is also used to keep the submerged body in the desired mean position. This is done by determining the parameters I_{min} and I_{max} at each time step, as explained in the following: If the opening is delayed relative to a maximum (wave crest) the buoy will pull the plate upwards, and if it is delayed relative to a minimum (wave trough) the buoy will push the plate downwards. We introduce $s_{r,max}$, which is the most extreme excursion of the piston $(s_p(t) - s_b(t))$ in positive direction since the last time the valve was closed after a time interval when the piston was moving upwards, and $s_{r,min}$, which is the most extreme excursion of the piston in negative direction since the last time the valve was closed after a time interval when the piston was moving downwards. If $s_{r,max} < 1.5$ m, we choose $I_{max} = 70000$ Ns, and if $s_{r,max} > 1.5$ m $I_{max} = (2.5\text{ m} - s_{r,max}) \cdot 70000$ Ns/m, but not below 20000 Ns. In addition the

present excursion is taken into consideration, so that if $(s_p(t) - s_b(t)) < 1.0$ m I_{max} is increased by 3000 Ns, if $(s_p(t) - s_b(t)) < 0.5$ m I_{max} is increased by 6000 Ns, and if $(s_p(t) - s_b(t)) < 0$ m I_{max} is increased by 9000 Ns. If $s_{r,min} > -1.5$ m, we choose $I_{min} = -80000$ Ns, and if $s_{r,min} < -1.5$ m, $I_{min} = -(2.5 \text{ m} + s_{r,min}) \cdot 80000$ Ns/m, but not above -20000 Ns. In addition the present excursion is taken into consideration, so that if $(s_p(t) - s_b(t)) > -1.0$ m I_{min} is reduced by 5000 Ns, if $(s_p(t) - s_b(t)) > -0.5$ m I_{min} is reduced by 10000 Ns, and if $(s_p(t) - s_b(t)) > 0$ m I_{min} is reduced by 15000 Ns. This procedure has been developed empirically by running the program for different wave condition and changing the parameters to maximise the power production, while at the same time trying to keep the excursion within the design limits.

The opening instant is determined as follows. The first three extrema of $I_{int}(t')$ are located, starting at $t' = t + T_0/4$. This is done by examining the time derivative of $I_{int}(t')$. If there are less than three extrema in the interval where the excitation force is known, the remaining extrema are assumed to be after the end of the interval. If the first and third extremum, which are in the same direction, are separated by more than a certain predetermined time interval (in this case half the natural period of the buoy ($T_0/2$) has been used) the first extremum is chosen as input to the control. If the extrema are close, it will not be possible for the buoy to move significantly in this ("interextreme") time interval, and either the first or third extremum is chosen as input to the control. If the first extremum is a maximum, the extremum with highest maximum value (usually positive) is chosen, or if the first extremum is a minimum the extremum with lowest minimum value (usually negative) is chosen. The time of the extremum used for the control, is denoted t_{extr} .

It should then be determined when the valve should be opened relative to the extremum, and we will first consider a maximum. If $I_{int}(t + T_0/4) < I_{min}$ and the derivative of I_{int} is positive for $t' = t + T_0/4$, the opening has been delayed relative to the previous minimum and it is searched for the first opening instant where $I_{int}(t_{open} + T_0/4) > I_{min}$. Otherwise, if $I_{int}(t_{extr}) < I_{max}$ the opening instant is set to $t_{open} = t_{extr} - T_0/4$, that is we will have coinciding extremum of velocity and excitation force, or if $I_{int}(t_{extr}) > I_{max}$ it is searched for the first opening instant where $I_{int}(t_{open} + T_0/4) < I_{max}$.

If the first extremum is a minimum the following procedure is used. If $I_{int}(t + T_0/4) > I_{max}$ and the derivative of I_{int} is negative for $t' = t + T_0/4$, the opening has been delayed relative to the previous maximum and it is searched for the first opening instant where $I_{int}(t_{open} + T_0/4) < I_{max}$. Otherwise, if $I_{int}(t_{extr}) > I_{min}$ the opening instant is set to $t_{open} = t_{extr} - T_0/4$, that is we will have coinciding extremum of velocity and excitation force, or if $I_{int}(t_{extr}) < I_{min}$ it is searched for the first opening instant where $I_{int}(t_{open} + T_0/4) > I_{min}$.

When the opening instant, t_{open}, has been determined, it should be determined if the valve should be open during the next time step. If $t < t_{open}$ the valve remains closed, because it is to early to open it. Otherwise, an approximation to what the acceleration of the buoy and plate will be, if the valve were opened, is computed. This is done by assuming that the cylinder pressure will be equal to the pressure in accumulator *A* (see figure 4), when the valve is opened. If the piston starts moving in the desired direction, that is, downwards if the extremum of the excitation force is a maximum and upwards if the extremum is a minimum, the valve is opened, otherwise it remains closed.

If the valve is open when entering the procedure, it should be determined whether the valve should remain open, or be closed. If it is less than a certain time interval since the valve was opened, in the present case 0.2 s is used, it remains open (1). This is done so that the piston should have time to start moving in the desired direction, and since it is not

desirable that the valve should open and close too often. Afterwards, the valve is closed when the velocity of the piston relative to the cylinder ($u_p(t') - u_b(t')$) changes sign, which is also when the excursion of the piston relative to the cylinder (or plate relative to buoy) has its extreme value. In this way the flow through the valve is approximately zero at the instant of closing the valve.

References

1. Budal, K.: Floating structure with heave motion reduced by force compensation. *Proc. 4th Int. Offshore Mechanics and Arctic Engineering Symp.*, Vol. 1, pp. 92-101, ASME, New York, 1985

2. Eidsmoen, H.: *On theory and simulation of heaving-buoy wave-energy converters with control*. Dr.ing. thesis 1995:126, Division of Physics, Norwegian Institute of Technology, Trondheim, Norway, 1995

3. Budal, K., Falnes, J., Kyllingstad, Å., and Oltedal, G.: Experiments with point absorbers. *Proc. First Symp. on Wave Energy Utilization*, Gothenburg, Sweden, pp. 253-282, 1979

4. Greenhow, M.J.L., Rosen, J.H., and Reed, M.: Control strategies for the Clam wave energy device. *Applied Ocean Research*, Vol. 6, No. 4, pp. 197-206, 1984

5. Budal, K. and Falnes, J.: Optimum operation of improved wave-power converter. *Marine Science Communication*, 3(2), pp. 133-150, 1977

6. Nebel, P.: Maximizing the efficiency of wave-energy plant using complex-conjugate control. *Proc. Instn. Mech. Engrs.*, Vol. 206, pp. 225-236, 1992

7. Pizer, D.: Maximum wave-power absorption of point absorbers under motion constraints. *Applied Ocean Research*, Vol. 15, No. 4, pp. 225-236, 1993

8. Salter, S.H., Jeffery, D.C., and Taylor, J.R.M.: The architecture of nodding duck wave power generators. *The Naval Architect*, Jan 1976, pp. 21-24

9. Nichols, N.K., Falcão, A.F. de O., and Pontes, M.T.: Optimal phase control of wave power devices. *Wave Energy*, Institute of Mechanical Engineers, London, pp. 41-46, 1991

10. Korde, U.A.: On the control of wave energy devices in multi frequency waves. *Applied Ocean Research*, Vol. 13, No. 3, pp. 132-144, 1991

11. Budal, K., Falnes, J., Iversen, L.C., Hals, T. and Onshus, T.: Model experiments with a phase-controlled point absorber. *Sec. Int. Symp. on Wave & Tidal Energy*, September 23-25, 1981, BHRA Fluid Engineering Centre, Bedford, U.K., pp. 191-206

12. Iversen, L.C.: Numerical method for computing the power absorbed by a phase-controlled point absorber. *Applied Ocean Research*, Vol. 4, No. 3, pp. 173-180, 1982

13. Sarmento, A.J.N.A., Gato, L.M.C., and Falcão, A.F. de O.: Turbine controlled wave energy absorption by oscillating water column device. *Ocean Engng.*, Vol. 17, No. 5, pp. 481-497, 1990

14. Hoskin, R.E., Count, B.M., Nichols, N.K., and Nicol, D.A.C.: Phase Control for the Oscillating Water Column. *Hydrodynamics of Ocean Wave-Energy Utilization* (Evans, D.V. and Falcão, A.F. de O. editors), IUTAM Symp., Lisbon, Portugal (1985), Springer Verlag, Berlin, 1986, pp. 257-268

15. Hoskin, R.E., Nichols, N.K., Nicol, D.A.C., and Count, B.M.: Latching Control of a Point Absorber. *Water for Energy*, BHRA Fluid Engineering Centre, Bedford, U.K., pp. 317-330, 1986

16. Hoskin, R.E. and Nichols, N.K.: Optimal strategies for phase control of wave energy devices. *Utilization of Ocean Waves*, American Society of Civil Engineers, pp. 184-199, 1987

17. Hoskin, R.E.: *Optimal control techniques for wave power generation.* Ph.D. Thesis, Dept. of Mathematics, University of Reading, U.K., 1988

18. Eidsmoen, H.: Optimum control of a floating wave-energy converter with restricted amplitude. *Proc. 14th Int. Conf. on Offshore Mechanics and Offshore Engineering*, Vol. 1A, pp. 139-146, ASME, 1995

19. Eidsmoen, H.: Hydrodynamic parameters for a two-body axisymmetric system. *Applied Ocean Research*, vol. 17, No.2, pp. 103-115, 1995

20. Cummins, W.E.: The Impulse Response Function and Ship Motions. *Schiffstechnik*, Vol. 9, pp.101-109, 1962

21. Morison, J.R., O'Brien, M.P., Johnson, J.W. and Schaaf, S.A.: The Force Exerted by Surface Waves on Piles. *Petrol. Trans., Am. Inst. Mining Engrs.*, Vol. 189, pp. 149-154, 1950

22. Keulegan, G. H. and Carpenter, L.H.: Forces on Cylinders and Plates in an Oscillating Fluid. *Journal of Research of the National Bureau of Standards*, Vol. 60, No. 5, pp. 423-440, May 1958

23. See e.g. Press, W.H, Teukolsky, S.A., Vetterling, W.T. and Flannery, B.P.: *Numerical Recipes in C.* Cambridge University Press, New York, 1992

24. Pierson, W.J. Jr. and Moskowitz, L.: A Proposed Spectral Form for Fully Developed Wind Seas Based on the Similarity Theory of S.A. Kitaigorodskii. *J. Geophys. Res.*, Vol. 69, No. 24, 1964, pp. 5181-5190

25. Eidsmoen, H.: Simulation of a heaving-buoy wave-energy converter with phase control. *The Second European Wave Power Conference. Proceedings of an International Conference held in Lisbon, Portugal, 8 to 10 November 1995* (edited by G. Elliot and K. Diamantaras), (ISBN 92-827-7492-9, 1996), pp. 281-288.

26. Hasselmann, K. et al.: Measurements of wind-wave growth and swell decay during the Joint North Sea Wave Project (JONSWAP). *Deutsches Hydrograph. Zeitschrift*, No. 12, 1973

27. Newman, J.N.: *Marine Hydrodynamics.* MIT Press, 1977, pp. 314-317

28. Krogstad, H.E.: *Statistikk over bølgeparametre.* Continental Shelf Institute (IKU), Trondheim, Norway, 1978

29. Lillebekken, P.M. and Falnes, J.: *Wave-energy conversion by arrays of controlled point absorbers with restricted heave amplitude.* Internal note, Division of Physics, Norwegian Institute of Technology, University of Trondheim, Norway, 1995 (submitted to the EU/JOULE project "Offshore Wave Energy Converters OWEC-1")

30. Evans, D.V. and McIver, P.: Added mass and damping of a sphere section in heave. *Applied Ocean Research*, Vol. 6, No. 1, pp. 45-53, 1984

31. Falnes, J.: On non-causal impulse response functions related to propagating water waves. Accepted for publication in *Applied Ocean Research.*

32. Falnes, J. and McIver, P.: Surface wave interaction with systems of oscillating bodies and pressure distributions. *Applied Ocean Research*, Vol. 7, No. 4, pp. 225-234, 1985

33. Budal, K. and Falnes, J.: *Kraftbøye. System E*. Internal note, Division of Physics, NTH, 1978 (Included as appendix in Falnes, J.: *Preliminary design and model test of a wave power converter : Budal's 1978 design type E.* Internal note, Division of Physics, NTH, University of Trondheim, Norway, 1993)

34. Salter, S.H. and Rampen, W.: The Wedding-Cake Multi-eccentric Radial Piston Hydraulic Machine with Direct Computer Control of Displacement Applied to Wave Energy Devices. *Proc. European Wave Energy Symp.*, Edinburgh, Scotland, U.K., pp. 89-195, 1993